

1 **The coupling between hydrology, the development of the active
2 layer and the chemical signature of surface water in a
3 periglacial catchment in West Greenland**

4 Johan Rydberg^{1*}, Emma Lindborg^{2, 3}, Christian Bonde⁴, Benjamin M. C. Fischer⁵, Tobias
5 Lindborg^{6, 3}, Ylva Sjöberg^{7, 4, 1}

6 ¹Department of Environmental Science, Umeå University, Linnaeus väg 6, 901 87 Umeå, Sweden

7 ²DHI Sweden AB, Svartmangatan 18, 111 29 Stockholm, Sweden

8 ³Blackthorne Science AB, Slånbarstigen 36, 125 56 Älvsjö, Sweden

9 ⁴Department of Geosciences and Natural Resource Management, and Center for Permafrost, University of
10 Copenhagen, Øster Voldgade 10, 1350 København K, Denmark

11 ⁵Department of Earth Sciences, Uppsala University, Villavägen 16, 752 36 Uppsala, Sweden

12 ⁶Swedish Nuclear Fuel and Waste Management Company (SKB), Box 3091, 169 03 Solna, Sweden

13 ⁷Department of Physical Geography and the Bolin Centre for Climate Research, Stockholm University, 106 91
14 Stockholm, Sweden

15 Correspondence to: Johan Rydberg (johan.rydberg@umu.se)

16 **Abstract.** ~~An important factor for controlling~~ the chemical signature of surface water is ~~the~~ the interactions with soil
17 particles and groundwater. In permafrost landscapes, ground ice restricts groundwater flow, which implies a
18 limited influence of processes such as weathering on the chemical signature of the runoff. The aim of this study
19 was to examine how freeze-thaw processes, hydrology and water age interact to shape the chemical and stable
20 hydrogen and oxygen isotopic signature of surface water in a catchment in West Greenland. Measuring runoff in
21 remote catchments is challenging, and therefore we used a validated hydrological model to estimate daily runoff
22 over multiple years. We also applied a particle tracking simulation to determine groundwater ages, and used data
23 on stable isotopic and chemical composition from various water types – including surface water, groundwater,
24 lake water and precipitation – spanning from early snowmelt to ~~the end of the thawed season~~. Our results show
25 that groundwater ~~age~~ generally ~~is less~~ than one year and rarely exceeds four years. ~~total runoff is dominated by~~
26 ~~groundwater, and overland~~ flow is restricted to the snowmelt period and after heavy rain events. Monitoring of
27 thaw rates in the active layer indicates a rapid thawing in connection with running water, and meltwater from
28 ground ice quickly becomes an important fraction of the runoff. Taken together, our data suggest that even in
29 continuous permafrost landscapes with thin active layers and an absence of truly old ~~and~~ mobile groundwater, soil
30 processes exert a strong influence on the chemical and stable isotopic signature of runoff, similar to what has been
31 observed in other climatic settings.

32

33

Deleted: T

Deleted: influenced by

Deleted: late in the hydrological active season

Deleted: is

Deleted: younger

Deleted: .

Deleted: o

Deleted: , while runoff is dominated by groundwater

42 **1 Introduction**

43 The water that falls as precipitation carries a signature that reflects the chemical conditions in the atmosphere.
44 This chemical signature – or water quality – is subsequently altered as the water flows through a catchment, where
45 it interacts with water stored in the landscape, vegetation, soil particles and bedrock (Sprenger et al., 2019). The
46 resulting water quality not only determines the ecological and chemical status of local and downstream aquatic
47 systems (EU, 2002), it can also shine light on hydrological pathways and biogeochemical cycling within
48 catchments (Fischer et al., 2015; Lidman et al., 2014; Lyon et al., 2010a; Jutebring Sterte et al., 2022). Knowledge
49 regarding the interplay between soil processes and water also helps us understand how future changes in, e.g.,
50 climate, might affect hydrological pathways and the biogeochemical cycling of elements (Frey and McClelland,
51 2009; Vonk et al., 2015; Winnick et al., 2017).

52 Water transit time in a catchment depends on several factors, including the thickness of the regolith and the size
53 of the groundwater aquifer, and groundwater transit times range from days in the shallow layers (0–10 cm) to
54 several hundreds of years as depth increases (Condon et al., 2020). In high latitude regions, the long and cold
55 winters restrict the flow of water during a considerable part of the year. Instead a large proportion of the annual
56 precipitation is released as runoff during the short and intense snowmelt period (Bring et al., 2016; Johansson et
57 al., 2015a). Not only is the runoff during the snowmelt period high, the presence of ground ice can also limit the
58 interaction between the meltwater and deeper soil layers (Bosson et al., 2013; Johansson et al., 2015a). Because
59 of this, the meltwater that reaches a stream can, at least during the initial phase of the snowmelt period, be expected
60 to have a short transit time and mostly reflect the chemical signature of the melting snow (Chiasson-Poirier et al.,
61 2020).

62 When the upper soil layers thaws, meltwater from snow can infiltrate the ground surface and interact with
63 decomposing plant material in the organic horizon and mineral soil particles (Cai et al., 2008; Quinton and
64 Pomeroy, 2006). The thawing of progressively deeper soil layers also enables recent snowmelt water to interact
65 and mix with older water that was stored in the ground prior to the onset of the snowmelt period (i.e., pre-event
66 water; Tetzlaff et al., 2018). A prerequisite for these interactions is that the ground thaws while the snowmelt
67 period is still ongoing. This is the case in forested catchments without permafrost in the boreal region, where
68 stream-water dissolved organic carbon (DOC) concentrations increase during the snowmelt period (Jutebring
69 Stere et al., 2018; Laudon et al., 2004). However, in adjacent wetland catchment, where the ice-rich peat results
70 in slower thaw rates, the limited infiltration of snowmelt water results in a decrease in DOC during the snowmelt
71 period and shorter transit time of the water (Jutebring Sterte et al., 2018; Laudon et al., 2004; Lyon et al., 2010b).

72 In permafrost regions the groundwater storage can be expected to be smaller than in areas without permafrost
73 because the upper part of the ground that thaws each summer, i.e., the active layer, constitutes a much thinner
74 groundwater aquifer than what is common in systems without permafrost (Petrone et al., 2016). A consequence
75 of a limited groundwater storage is that the system can become more responsive to changes in the source of the
76 water. This can, e.g., be seen in a study of a polygonal tundra site in Alaska where there are no signs of any
77 snowmelt water in the soil during the summer (Throckmorton et al., 2016). A quick response to change is also
78 evident in a catchment-scale study conducted in the Northwest Territories in Canada, where streamflow during
79 the snowmelt period, when water transit times were short, was primarily governed by the input from snowmelt
80 (Tetzlaff et al., 2018). Over the course of the summer period there was a significant increase in the contribution
81 of water from the subsurface system and riparian zones, and water transit times progressively increased to longer

Deleted: the

Deleted: Water transit time through

Deleted: things,

Deleted: depth

Deleted: stores

Deleted: addition to storage characteristics

Deleted: in high latitude regions

Deleted: ,

Deleted: resulting in the snowmelt

Deleted: period being the single most important event of the hydrological year ...

Deleted: high

Deleted: but

Deleted: meltwater also flows through a system where

Deleted: s

Deleted: the

Deleted: particles

Deleted: That is

Deleted: the water that reaches a stream can be expected to

Deleted: As

Deleted: in deeper layers

Deleted: hat t

Deleted: upper part of the ground thaws also means that

Deleted: can

Deleted: event

Deleted: between snowmelt water and soil particles

Deleted: s

Deleted: boreal

Deleted: A result of this

Deleted:), where no traces of snowmelt water were found in soil water collected during summer.

Deleted: Similarly,

Deleted: Tetzlaff et al. (2018) reported that during the snowmelt period, ...

Deleted: ,

Deleted: and the transit times were short

Deleted: then

119 than 1.5 years at the end of the summer. This suggests that, during the snowmelt period, the presence of
120 impermeable ground ice that thaw slowly, results in most of the meltwater leaving the system as overland flow or
121 evaporation. In time, however, the thaw in the active layer activate deeper flow paths and lead to the release of
122 older pre-event water.
123 Thaw rates in the active layer are therefore important for both water transit times and the chemical signature of
124 the water, but because the thaw rates are controlled by more than air temperatures they can be difficult to predict.
125 On the one hand, the high latent heat of ground ice implies that more ice-rich (wetter) soils can be expected to
126 thaw slower (Clayton et al., 2021). On the other hand, ice-rich (wet) soils have a higher thermal conductivity than
127 dry soils and could thereby thaw quicker (Clayton et al., 2021). In addition, running water can contain considerable
128 amounts of heat energy that could influence the thaw process (Sjöberg et al., 2016). This advective heat transfer
129 suggests that areas in close connection to running water, e.g., surface-water flow paths, could thaw faster than the
130 typically drier areas further away from running water. The microtopography could also influence the distribution
131 of snow, and because snow insulates the ground during winter, it can be expected that low-lying areas will have
132 higher ground temperatures in spring (O'Connor et al., 2019). Taken together this means that it can be difficult to
133 predict thaw rates, but that we can expect significant differences between lower lying wet areas and more elevated
134 dry areas.
135 The snowmelt period is followed by a warmer summer period with less water moving through the catchment and
136 a progressively thicker thawed layer that allows for deeper and longer groundwater flow paths. In boreal systems
137 without permafrost, deeper flow paths, increased water age and a greater influence of groundwater generally lead
138 to a chemical signature more influenced by soil processes (e.g., weathering and decomposition of organic matter
139 (OM); Jutebring Sterte et al., 2021a). Higher temperatures also lead to increased evaporation, which concentrates
140 both elements supplied via atmospheric deposition and elements supplied through weathering and decomposition
141 (Alvarez et al., 2015). Taken together we could expect that surface water collected during the summer, when
142 transit times are longer, should have a very different chemical signature compared to water from the snowmelt
143 period. However, in areas with continuous permafrost the active layer can be less than a meter even when fully
144 developed in late summer (Petrone et al., 2016). That is, even the deepest flow paths are very shallow compared
145 to boreal systems without permafrost (Jutebring Sterte et al., 2021b). This implies that the average age of the
146 runoff in an area with continuous permafrost should be younger, that the flow paths should be shorter and that
147 most of the water leaving the system should have had a more limited time to interact with the soil particles
148 compared to boreal areas without permafrost (Tetzlaff et al., 2018). Hence, the question remains to what extent
149 the water chemistry in areas with continuous permafrost is affected by – and reflects – processes in the catchment,
150 or if the water leaves the system too rapidly to pick up any discernible signature from the catchment.
151 Knowledge regarding how the chemical signature is altered as the water moves through the catchment is essential
152 to make reliable predictions regarding how future changes in the climate will affect biogeochemical cycling
153 especially in Arctic areas with continuous permafrost. However, despite being located in a global climate hotspot
154 (Rantanen et al., 2022) the processes influencing the water quantity and quality in the Arctic remain poorly
155 understood, partly because of a declining research infrastructure (Laudon et al., 2017) and a limited availability
156 of spatiotemporal data due to the region's remote location and extreme climatic conditions (Tetzlaff et al., 2018;
157 Throckmorton et al., 2016). In order to better understand how flow paths, water age and chemical signatures
158 covary over different time scales in a periglacial landscape with continuous permafrost we have used a well-

Deleted: with a significant increase in the contribution of water from the subsurface system and riparian zones

Deleted: slow thaw rates of this ice

Deleted: are activated

Deleted: that was stored prior to the onset of the snowmelt becomes more important for the chemical signature of the runoff

Deleted: As indicated above, t

Deleted: are not only a consequence of air temperatures

Deleted: also plays an important role, which

Deleted: s

Deleted: wetter areas and

Deleted: In addition,

Deleted: m

Deleted: s

Deleted: how

Deleted: and

Deleted: the thickness of the thawed layer vary spatially across the landscape...

Deleted: .

Deleted: After the intense

Deleted: s

Deleted: period

Deleted: and

Deleted: with

Deleted: those

Deleted: water

Deleted: is

Deleted: are

Deleted: has

Deleted: This

Deleted: k

Deleted: ,

Deleted: ,

Deleted: 1

193 studied catchment in West Greenland, i.e., the Two-Boat Lake catchment (Johansson et al., 2015b; Lindborg et
194 al., 2016; Lindborg et al., 2020; Petrone et al., 2016; Rydberg et al., 2023; Rydberg et al., 2016). A key novelty
195 of the present study is the coupling of field observations of water chemistry and thaw rates in the active layer with
196 a well-constrained, distributed, hydrological model (Johansson et al., 2015a). This approach allows us to address
197 the following specific research questions: i) can we observe any relationship between soil wetness and the thaw
198 rate in the active layer during the snowmelt period, ii) does the chemical signature and stable isotopic composition
199 of the runoff suggest that the thaw in the active layer is fast enough to allow the meltwater from snow to interact
200 with soil particles and pre-event water during the snowmelt period, iii) considering the dry conditions and the thin
201 aquifer, is the interaction with soil particles large enough to alter the chemical signature of the runoff, or do our
202 data suggest that other factors (e.g., atmospheric deposition and evapotranspiration) are more important for the
203 controlling the water quality of surface waters.

204 2 Methods

205 2.1 Study area

206 Two-Boat Lake (also referred to as SS903, lake area: 0.37 km²) and its terrestrial catchment (1.7 km²) are situated
207 in West Greenland (Lat 67.126° Long -50.180°), about 25 km east of the settlement of Kangerlussuaq (Fig. 1).
208 Even though the Greenland ice sheet is only about 500 m from the lake, it receives no direct input of glacial
209 meltwater from the ice sheet (Johansson et al., 2015a). Permafrost in the Two-Boat Lake catchment is continuous
210 and reaches down to about 400 m, except under the lake itself where a through talik has formed (Claesson Liljedahl
211 et al., 2016). Bedrock consists mostly of tonalitic and granodioritic gneisses (Van Gool et al., 1996) and is covered
212 by till or glaciofluvial deposits that are, in turn, overlain by a layer of eolian material in the valleys (Petrone et al.,
213 2016). The climate of this region is cold and dry, with a mean annual air temperature for the Two-Boat Lake
214 catchment of -4.4 °C (Johansson et al., 2015b). The mean annual precipitation for the period 2011-2013 was 270
215 mm yr⁻¹ (163-366 mm yr⁻¹) with about 40% falling as snow. The high evapotranspiration in the terrestrial part of
216 the catchment (138-199 mm yr⁻¹) results in a relatively low runoff to the lake (25-159 mm yr⁻¹), of which about
217 half is associated with the snowmelt period (Johansson et al., 2015a). There are no permanent streams or confined
218 stream channels in the catchment. Instead, surface runoff occurs in small (typically <0.5m wide), temporary
219 surface streams that are active only during high runoff situations, particularly the snowmelt period (Johansson et
220 al., 2015a). The vegetation zone in the area can be characterised as polar tundra or steppe (Bush et al., 2017;
221 Böcher, 1949), and the vegetation of the Two-Boat Lake catchment has been described in detail by Clarhäll
222 (2011). Between 2010 and 2019 the catchment was the study site of the Greenland Analogue Surface Project
223 (GRASP), which was funded by the Swedish Nuclear Fuel and Waste Management Company (SKB). During
224 GRASP, data regarding meteorology, hydrology, Quaternary deposits, vegetation cover and active layer thickness
225 were collected together with samples from soils, groundwater, surface- and lake water for chemical analysis. All
226 data collected during GRASP have been thoroughly described in three publications (Johansson et al., 2015b;
227 Lindborg et al. 2016; Petrone et al. 2016), and the datasets are available at www.pangaea.de (SI-Table 1). For this
228 study we have focused on a sub-catchment (0.6 km²) in the northern part of the Two-Boat Lake catchment (Fig.
229 1).
230

Deleted: the main factor in driving
Deleted: composition
Deleted: during the unfrozen season
Deleted: samples
Deleted: there are other important factors that contribute to shaping t...
Deleted: chemical signature of the water

Deleted: the
Deleted: is relatively low
Deleted: and
Deleted: most of the runoff

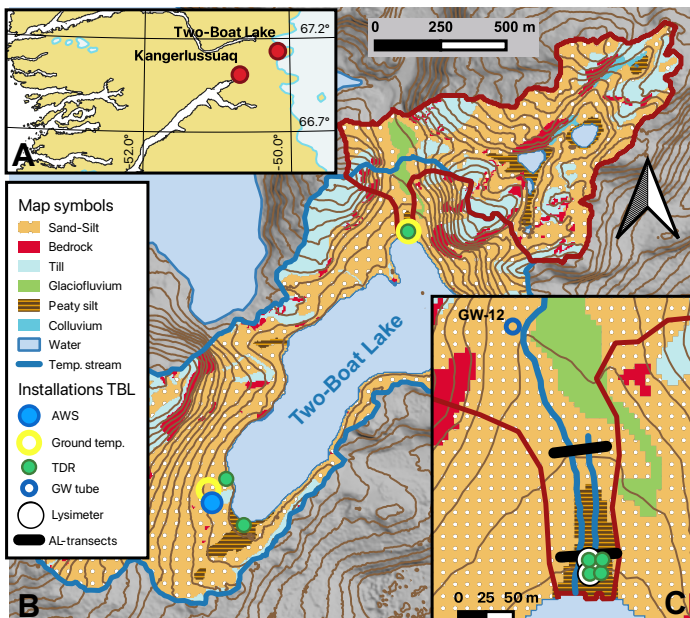


Figure 1. Map showing the location of the Two-Boat Lake catchment within West Greenland (panel A). Panel B shows a map over the Quaternary deposits for the entire Two-Boat Lake catchment (peaty silt corresponds to wetter areas), including the location of the automated weather station (AWS), ground temperature loggers, and TDR-installations. The red outline corresponds to the sub-catchment used for this study, while the blue outline marks the original catchment area used by Johansson et al. (2015a). Panel C shows a close-up of the lower part of the studied sub-catchment, including the two transects that were used to monitor the thaw in the active layer (AL) during spring 2017 and the two temporary streams that were active during this period. It also shows the location of the groundwater well (GW-12) and two lysimeter installations that were used as observation points in the particle tracking simulation, as well as the four TDR depth profiles in the sub-catchment. The digital elevation model used to create the contour lines (10-m contour intervals) and the regolith map were developed within the GRASP-project and are described in detail in Petrone et al. (2016).

2.2 Modelling

2.2.1 Hydrological modelling

During GRASP, Johansson et al. (2015a) used the modelling system MIKE SHE to develop a distributed numerical hydrological model for the Two-Boat Lake catchment for the period 2011-2013 (i.e., original modelling period). Here we have extended the modelling period to also cover 2013-2019 (i.e., extended modelling period). The model uses meteorological data collected by an automated weather station (AWS) in the Two-Boat Lake catchment (Fig. 1) and has been thoroughly validated using on-site measurements of several hydrologic variables. The model domain has a horizontal resolution of 10x10 m, and covers the entire catchment, as well as the area directly downstream of the lake outlet (to avoid boundary effects). Vertically, the model is composed of four 25-

Deleted: :

Deleted: regolith

Deleted: of

Deleted: AL-

268 cm thick layers in the seasonally thawed active layer (top 100 cm), where water flow occurs seasonally, and four
269 layers in the underlying permafrost (1-200 m depth), where water mobility is extremely low due to the frozen
270 conditions (see Johansson et al. 2015a for details on model setup and validation).

271 Observed daily precipitation and potential evapotranspiration (PET, calculated based on temperature, wind speed,
272 air humidity and radiation from the AWS) are applied as the upper boundary condition. The actual total
273 evapotranspiration (as sublimation, interception, evaporation from open water and soil, and transpiration) is
274 calculated during the simulation as a result of the relation between the PET and the water availability. For the
275 remainder of the article, we will refer to the joint effect of sublimation, interception, evaporation and transpiration
276 as evapotranspiration. If the air temperature is below zero, the precipitation accumulates in the catchment as snow
277 (which is subsequently released during spring). When the air temperature is above zero the water from
278 precipitation can either leave as surface run-off or infiltrate the ground (the same applies for water from melting
279 snow and ice). The subsurface is composed of an unsaturated zone from which water can evaporate via the soil
280 matrix, transpire through plant roots, percolate to the saturated zone or remain in storage. This unsaturated zone
281 varies in thickness depending on the depth of the simulated groundwater table. In the saturated zone, below the
282 groundwater table, water can move vertically and horizontally as simulated by Darcy's law. The water flow in
283 and between each model compartment (river/streams, overland, unsaturated zone, saturated zone) is quantified
284 during the simulation and constitutes the basis for the calculation of the catchment water balance (Johansson et
285 al. 2015a).

286 Because MIKE SHE does not itself simulate freeze-thaw processes (i.e., permafrost), the impact of freeze-thaw
287 processes on the hydrological flow in the active layer and permafrost was parameterized by spatially and
288 temporally varying the hydraulic properties (hydraulic ~~conductivity~~, surface roughness and infiltration capacity)
289 of the ground substrates based on the observed ground temperatures at different depths and locations in the
290 catchment. By using this approach, MIKE SHE handles permafrost by simulating the hydrological consequences
291 of frozen and thawed conditions rather than simulating ground temperatures (Bosson et al., 2013). That is, water
292 mobility in the subsurface zones is effectively restricted when the ground is frozen. For more details regarding
293 the model setup and validation, please refer to Johansson et al. (2015a).

294 Code developments in MIKE SHE between the original and the extended ~~modelling period~~ resulted in two model
295 versions and associated evaluation periods. For the original 2010-2013 period, we used the output from the
296 original modelling run made by Johansson et al. (2015a). For the ~~extended~~, 2013-2019, period the same model
297 was used, but with the inclusion of an additional catchment area (Fig. 1). This additional area only contributes
298 runoff to the lake during high flow situations, e.g., during the snowmelt period or after periods with intense rain,
299 and it is not connected to the rest of the catchment via a predefined stream network in the model (and was therefore
300 excluded for the original modelling period). When ponded water accumulates in this area, it is routed downhill as
301 overland flow or infiltrated to reach downstream areas of the catchment as shallow groundwater flow.

302 2.2.2 Particle tracking simulation to estimate groundwater age

303 In order to estimate the age of the water in the saturated zone of the studied sub-catchment we used the particle
304 tracking module in MIKE SHE together with the numerical hydrological model described above (Fig. 1). This
305 module adds virtual "particles" to the water that enters the saturated zone. These particles then move
306 (conservatively) with the water through the saturated zone until they leave the saturated zone ~~and enter~~ the lake,

Deleted: conductiviti

Deleted: es

Deleted: , 2015b

Deleted: model

Deleted: model run

Deleted: for the present study

Deleted: of the hydrological model

Deleted: into

315 a temporary surface stream, standing surface water, the unsaturated zone or reach a model boundary. Based on
316 the time when they entered the saturated zone and when they reached one of the three observation points it is
317 possible to get an estimate of the age of the groundwater (Fig. 1).
318 The MIKE SHE particle-tracking module releases particles along the established 3D flow field in the saturated
319 zone only. The number of particles released was flow-weighted, i.e., the more water that enters the saturated zone
320 during a certain period, the more particles were released during that period. In this case one particle was released
321 for each millimetre of added water. Once a particle leaves the saturated zone, the particle is removed from the
322 simulation. To ensure enough time for most particles to leave the saturated zone or reach the observation points,
323 particles were only released during the first year of the 100-year simulation and the hydrological model (i.e., the
324 MIKE SHE hydrological model described above) was cycled to create a 100-year simulation using the
325 meteorological conditions for 2016-2019. Groundwater age, i.e., the transit time in the saturated zone, was then
326 estimated by noting the date the particle entered the saturated zone and the date when the particle reached an
327 observation point (i.e., one of the groundwater wells (GW-12) and the two lysimeter installations located within
328 the sub-catchment; Fig. 1). Each observation point was subdivided into three vertical layers in accordance with
329 the hydrological model (i.e., 0–25 cm, 25–50 cm, 50–75 cm).

Deleted: meteorological conditions

330 2.3 Sample collections and field measurements

331 2.3.1 Monitoring of thaw rates in the active layer

332 Between May 18th and May 31st 2017, the progress of thaw in the active layer was monitored using a steel rod
333 along two 50-m long transects (AL-transects; Fig. 1). Every second day (7 times in total) we measured the
334 thickness of the thawed layer in 0.5-m intervals along the transects. Each measurement spot was also classified as
335 wet (water table at or above the ground surface) or dry (water table more than 5 cm below the ground surface),
336 and we measured the depth of any surface water. Thaw rates were then calculated by dividing the change in thaw
337 depth between two consecutive monitoring dates by the time between the two dates. When measuring the thaw
338 depth care was taken not to walk on the measured transect and we avoided walking along the same path twice.
339 No visible signs of tracks or rilling were observed either during the intense monitoring period or during the entire
340 GRASP study period. Thaw rates for the whole monitoring period and for each spot along the transects were
341 calculated as the average thaw rate for the entire period.▼

Deleted: 1

342 2.3.2 Meteorology and ground temperatures

343 Air temperature and precipitation (as both rain and snow) were recorded using an automated weather station
344 (AWS) placed in the Two-Boat Lake catchment, and ground temperatures were measured at two locations in the
345 catchment using HOBO U12-008 sensors (Fig. 1; see Johansson et al., 2015b for further details). Based on time-
346 laps photos from the catchment, snow ablation and formation of snow drifts can be extensive. On a catchment
347 scale, we have assumed that these two processes cancel each other out, and that they result in no net gain or loss
348 of water to the catchment. Time Domain Reflectometry (TDR) sensors (Campbell Scientific, CS615 sensors
349 connected to a CR1000 data logger) were placed in three clusters, each consisting of either three or four depth
350 profiles with four sensors evenly distributed from 5-10 cm below the ground surface down to 40-50 cm (Fig. 1;
351 see Johansson et al., 2015b for further details).

355 **2.3.3 Estimate of the amount of ground ice**

356 To estimate the amount of water released from melting ground ice during the intense monitoring period of 2017,
357 we used the soil moisture content recorded by the TDR sensors in the sub-catchment at the time of freeze-up in
358 the fall of 2016. These data allowed us to estimate the ground ice content at different depths, and thus, estimate
359 the release of meltwater as the thaw progresses. This estimate should be considered as a minimum, because
360 moisture migration during winter could give a higher ice content in spring compared to the fall conditions. The
361 amount of water released from melting ground ice between May 18th and May 31st, 2017, was estimated based
362 on the water content linearly interpolated between observation depths (TDR sensors) and the maximum thaw
363 depth for each point along the transects at the end of the intense monitoring period.

364 **2.3.4 Collection of water samples and chemical analysis**

365 Precipitation (rain and snow; n=8 and n=13, respectively), surface water (n=31), soil water (groundwater wells
366 and zero-tension lysimeters, n=23 and n=22, respectively) and lake water (n=28) samples have been collected at
367 an irregular, low, frequency between 2010 and 2019 (Lindborg et al., 2016). Groundwater wells are fully screened,
368 and collects water from the entire thawed layer, while lysimeters collect water at discrete depths (i.e., either 15,
369 30 or 35 cm depth). The ceramic body of the lysimeters has a pore size of <1 μm and no additional filtering was
370 done. For other sample types, the majority were filtered in the field using 0.45 μm polycarbonate membrane filters
371 (two lake water and two surface water samples were analysed unfiltered). All samples were frozen after sampling
372 and were kept frozen until analysis. Water samples have been analysed for their elemental composition (n=129)
373 using Inductively-Coupled Plasma Sector-Field Mass Spectrometry (ICP-SFMS) at ALS in Luleå, and/or
374 dissolved organic carbon (DOC; n=62) using the NPOC-method at either Stockholm University (Dept. of
375 Ecology, Environment and Plant Science), ALS in Luleå or Umeå University (Dept. of Ecology and
376 Environmental Science). Please refer to Lindborg et al. (2016) for further details.

Deleted: -

Deleted: ground

Deleted: -

Deleted: or

Deleted: /

Deleted:

377 In addition to this low-frequency sampling, a number of samples were collected during the intense monitoring
378 period (i.e., between May 18th and May 31st, 2017). One set of samples was used for ICP-SFMS and DOC
379 measurements. This sample set consists of samples from where one of the temporary surface streams enters Two-
380 Boat Lake, the uppermost groundwater well (GW-12), one lysimeter (15-cm depth) and from melted snow (Fig.
381 1). A second set of samples was used for analysing stable water isotopic signatures (δD and $\delta^{18}\text{O}$). Surface water
382 was sampled every second day from two locations along a small temporary surface stream, that crossed the AL-
383 transects used to monitor the thaw depth. Snow was sampled from three locations in the sub-catchment, and water
384 from ground ice in the active layer was sampled in three locations along the temporary surface streams by thawing
385 pieces of frozen ground in plastic bags and sampling the meltwater. All samples were taken as duplicate samples
386 (field replicates), and the stable isotopic composition in each sample was analysed in triplicate (laboratory
387 replicates). Stable water isotopes in all water samples from the 2017 sampling were analysed at Stockholm
388 University using a Cavity Ring-Down Spectrometer (Picarro L2130-I, manufacturer's precision of $\delta\text{D}<0.1\text{‰}$ and
389 $\delta^{18}\text{O}<0.02\text{‰}$). The analysis scheme of Penna et al. (Penna et al., 2010) was adopted, and results were reported
390 as δ -values in per mille (‰) relative to Vienna Standard Mean Ocean Water (VSMOW). All calculations and
391 statistical treatments were made using the average stable isotopic composition of the laboratory replicates.

Deleted: simultaneously with

Deleted: the snowpack above the groundwater well

Deleted: s

Deleted: one of

402 **2.4 Data analysis**

403 **2.4.1 Principal component analysis**

404 To evaluate and visualize similarities and differences between different types of water samples the chemical data
405 from rain, snow, temporary surface streams, groundwater wells, lysimeters and the lake itself were subjected to a
406 principal component analysis (PCA). For temporary surface streams, groundwater wells and lysimeters only
407 samples from the studied sub-catchment were included. Prior to the PCA, elements for which the majority of
408 observations were below the reporting limit in all water types were removed. For the remaining elements all values
409 below the reporting limit were replaced with half the reporting limit, and the dataset was then converted to z-
410 scores (average=0; variance=1) to remove any effects of scaling. After an initial PCA, we also removed elements
411 with communalities <0.7, as well as two snow samples collected on the lake that had elemental concentrations
412 similar to lake water indicating that they had been contaminated by lake water (collected 2014-04-11). We also
413 removed a single sample from a groundwater well (GW-11, 2011-09-13) that had a disproportionately strong
414 influence on the outcome of the PCA. This resulted in a total of 35 elements and 65 observations (rain=8, snow=6,
415 surface water=7, groundwater=23, lake water=11). All principal components (PCs) with eigenvalues above one
416 were extracted, and a Varimax rotated solution was used.

Deleted: compartments

Deleted: and

Deleted: an

417 **2.4.2 Correlation analysis**

418 All statistical calculations for the comparisons between hydrological variables and the chemical signature were
419 performed using SPSS v.29 (www.IBM.com). Correlation coefficients were calculated as Pearson correlations
420 (denoted r) if both variables were normally distributed (according to a Shapiro-Wilk test) or Spearman rank
421 correlations (denoted r_s) if at least one variable was non-normally distributed. For all tests, a significance level of
422 0.05 was used. The majority of the runoff in the Two-Boat Lake catchment occurs as groundwater, and several of
423 the hydrological parameters reported from the model are highly correlated. Therefore, only the total runoff to the
424 lake and the proportion of deep groundwater were used for the correlation analysis (these two parameters show
425 no correlation to each other).

426 **3 Results**

427 **3.1 Hydrological modelling, 2013-2019**

428 The observed mean annual precipitation for the extended modelling period (i.e., 2013-2019) was 308 mm yr^{-1} ,
429 and it varied from a minimum of 247 mm yr^{-1} in 2014 to a maximum of 407 mm yr^{-1} in 2017. Based on the local
430 meteorological observations, the hydrological model estimates that, on average, two thirds (65%) of the
431 precipitation left the system as evapotranspiration (including sublimation), and the period from late April through
432 October was characterized by a precipitation deficit (i.e., precipitation minus evapotranspiration was less than
433 zero), whereas the winter period had a precipitation surplus. On an annual basis the modelled average net input
434 of water to the catchment (i.e., precipitation minus evapotranspiration) was 109 mm yr^{-1} , with a variation from 64
435 mm yr^{-1} (2018) to 170 mm yr^{-1} (2017). Viewed over the entire 2011-2019 period most of this excess water left the
436 terrestrial system as runoff (on average 98 mm yr^{-1}) and entered the lake.

Deleted: average

Deleted: (65%)

442 The snowmelt period was the dominant runoff event in all modelled years and most commonly the total runoff
443 peaked in early June (Fig. 2). During the early snowmelt period a substantial part of the runoff occurred as
444 overland flow directly to the lake (i.e., water that had been in limited contact with the subsurface), but for the
445 latter part of the snowmelt period and the summer season the runoff was dominated by groundwater discharging
446 directly to the lake or via temporary surface streams (Fig. 2). The exception to this pattern was 2018, when
447 overland flow also occurred late in the snowmelt period and during summer. On an annual basis overland flow
448 made up 7-52% of the annual runoff (average 28%), with 2016 and 2018 standing out from the other years with
449 about half the water leaving the catchment as overland flow.

450 Observed ground temperatures down to two meters depth show a clear seasonal pattern that became muted with
451 depth (Fig. 2). On average for the 2011-2018 period the maximum thaw depth, which occurred in August, reached
452 the temperature sensor at 75 cm. The thawed period at 25 cm started in late May (May 29th) and reached 50 cm
453 by mid-June (June 20th). The ground then stayed unfrozen for about four months and froze at 25 cm in late
454 September and at 50 cm in mid-October. That the deeper parts of the active layer (at 50 cm) stayed unfrozen for
455 almost a month after air temperatures dropped below zero degrees and the surface layers froze means that
456 groundwater flow could continue also after the ground surface had frozen.

Deleted: not been in

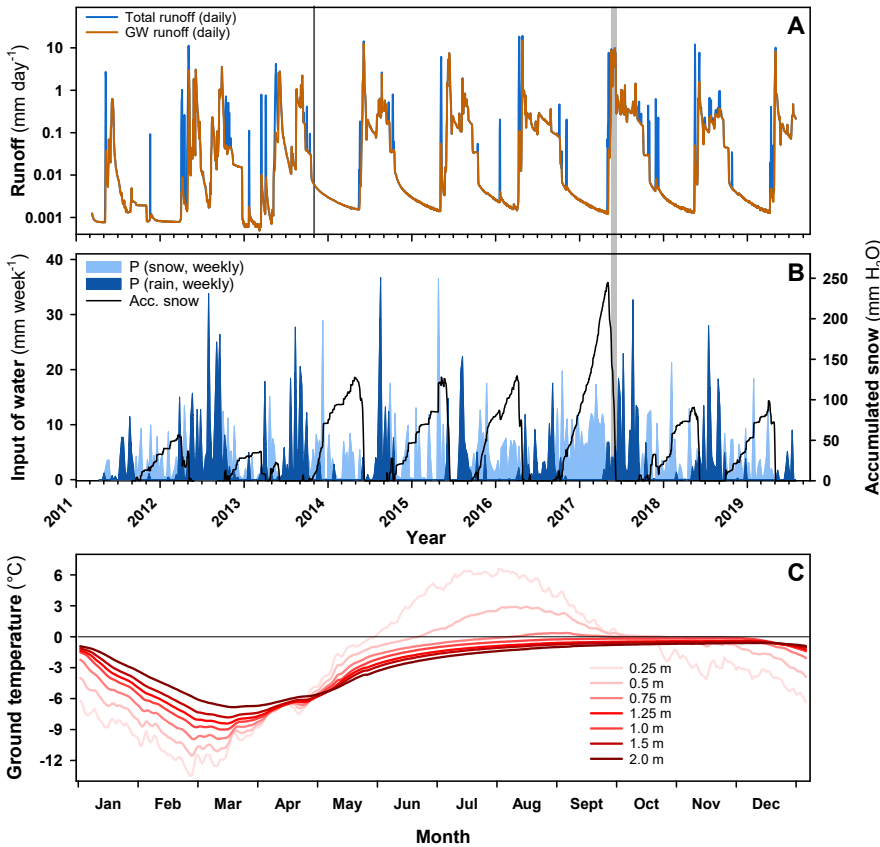
Deleted: ed

Deleted: a

Deleted: 0.

Deleted: months, and

Deleted: at 50 cm



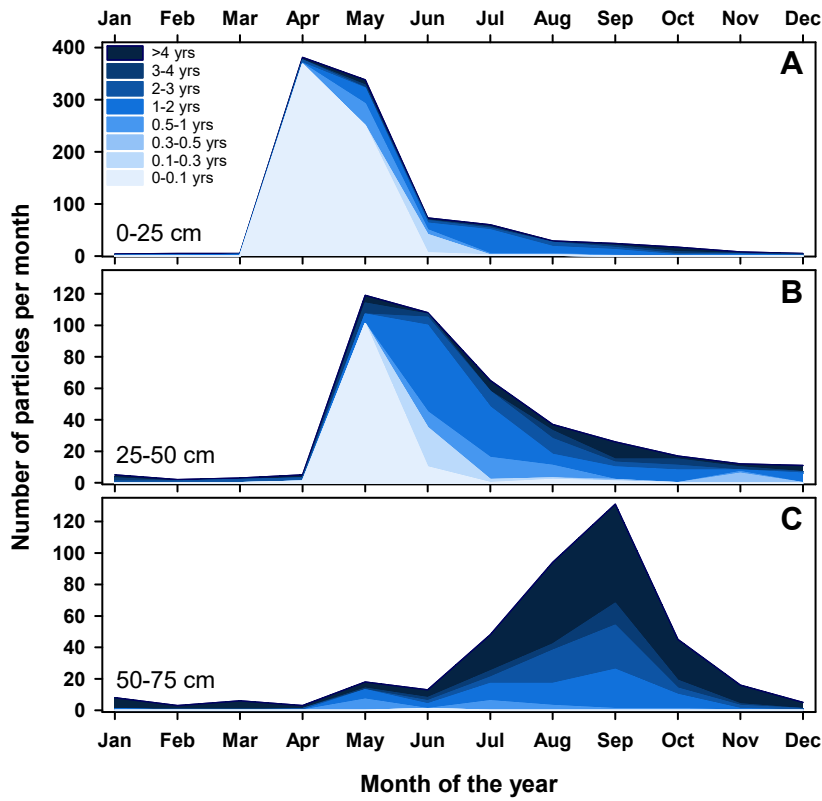
463
464 Figure 2. Panel A shows the modelled, daily runoff (total runoff and as groundwater) to Two-Boat Lake for the entire
465 modelling period (March 2011 to July 2019). The black vertical line denotes the division between the original modelling
466 period, presented in Johansson et al. (2015a), and the extended period (2013-2019). The grey vertical line indicates the
467 intense monitoring period in 2017. Panel B presents the observed weekly precipitation as snow (air temperature was
468 below zero) or rain for the Two-Boat Lake catchment. The black line represents the accumulation of water in the form
469 of snow in the catchment. The lower panel (C) shows the observed ground temperature (daily average for 2011-2018)
470 measured down to 2 m depth (cf. Fig. 1 for location)

Deleted: average

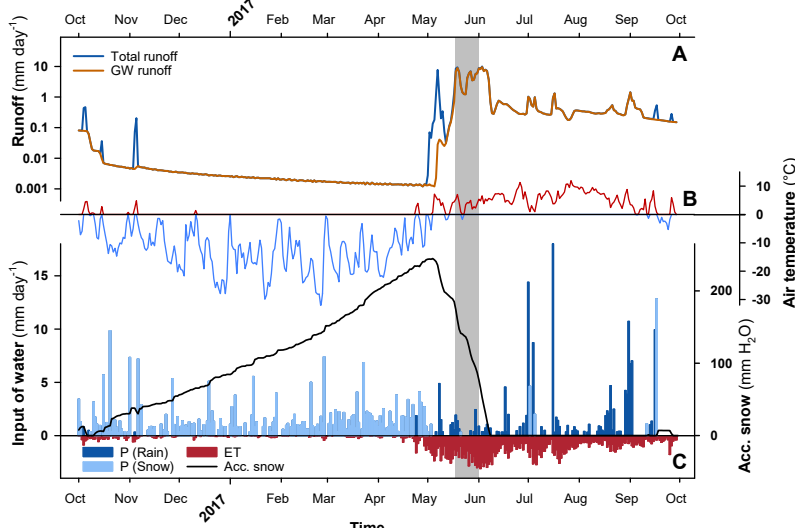
Deleted: run

Deleted: shaded

Deleted: area



Deleted: ,



483

484 **Figure 4. Modelled daily runoff from the hydrological model (A), observed daily air temperature (mean) for the Two-
485 Boat Lake catchment (B), and precipitation as snow or rain together with the loss of water through evapotranspiration
486 (including sublimation) for the period 2016-10-01 to 2017-09-30 (C). Water accumulated in the form of snow is
487 represented by the black line in panel C.** The intense monitoring period (May 18th to May 31st) is indicated by the
488 shaded area.

489 3.2 Particle tracking simulation and groundwater age

490 The particle tracking simulation suggests that most of the tracked particles moved through the uppermost layer of
491 the model (i.e., 0-25 cm; Fig. 3). From the start of the snowmelt period until the end of June—when most particles
492 are registered at the observation points—the 0-25 cm layer was dominated by very young water that generally
493 entered the saturated zone within the previous 3 months. As the unfrozen season progressed the average age of
494 the tracked particles increased in all three layers, and the flow also shifted to deeper flow paths when progressively
495 deeper layers thawed. In deeper layers the peak in the number of registered particles occurred later in the season
496 (May-June and September for 25-50 cm and 50-75 cm, respectively), and the particles registered in the deeper
497 soil layers also tended to have higher ages (Fig. 3). Almost all the particles that moved through the deepest part
498 of the active layer had spent more than a year in the saturated zone, and about two-thirds were older than two
499 years. It should be noted that particles only are released as water enters the saturated zone, hence, it is not possible
500 to track the age of water that was present in the saturated zone at the start of the particle tracking simulation, e.g.,
501 in permafrost. However, because the 100-year simulation does not include any warming trend (it repeatedly cycles
502 the 2016-2019 meteorological conditions), there is minimal release of water from thawing permafrost.

Deleted: average

Deleted: for the period 2016-10-01 to 2017-09-30

Deleted: for the same period

Deleted:

Deleted: same period

Deleted: ,

Deleted: as the unfrozen season progressed

Deleted: of the particles

Deleted: the ages only relate to

Deleted: Also,

Deleted: it does not include

Deleted: any

515 **3.3 Intense monitoring period in spring 2017**

516 During the winter 2016/2017, which preceded the intense monitoring period in late May 2017, the AWS in the
517 Two-Boat Lake catchment indicates that 260 mm of snow-water equivalent accumulated in the catchment.
518 According to the hydrological model 26.5 mm of this water was lost before the snowmelt period due to
519 sublimation and evaporation (Fig. 4). Based on the measured air temperature the hydrological model indicates
520 that the snowmelt started on April 30th, with about 8% of the snowmelt-associated runoff occurring before May
521 13th, mainly as overland flow directly to the lake (Fig. 4). This means that a substantial part of the accumulated
522 snowpack had already melted (or sublimated) at the beginning of the intense monitoring period (May 18th to May
523 31st), and snow patches were mainly confined to higher elevations in the catchment. Even so, multiple small
524 temporary surface streams were still observed across the catchment, and according to the hydrological model the
525 runoff remained high until June 10th. In contrast to during the early part of the snowmelt period, most water leaving
526 the terrestrial system, during the latter part of the intense monitoring period, had spent some time as groundwater
527 before entering a temporary surface stream or reaching the lake.
528 Time Domain Reflectometry (TDR) sensors installed in the sub-catchment showed a soil moisture content of
529 approximately 30% during soil freeze-up in the fall of 2016. Furthermore, the ground temperature sensors in the
530 sub-catchment showed that thawing of the ground at 5-cm depth started on May 10th, and that the thaw front
531 reached 15-cm depth on May 20th. The melting of ground ice in the active layer corresponds to a total water
532 release of at least 18 mm of water during the intense monitoring period, assuming that the recorded soil
533 temperatures and water content at the TDR sensors are representative for the entire sub-catchment. During the
534 intense monitoring period (May 18th to May 31st) there was also an input of a total of 7 mm of rain, with the largest
535 rainfall event of 0.8 mm occurring on May 30th.

536 **3.4 Thaw rates in the active layer**

537 At the start of the intense monitoring period (May 18th) the average thaw depth along the two AL-transects was
538 10.4 cm, and by the end of the period (May 31st) it had increased to 15.3 cm, but there was considerable variability
539 along the two transects. The progression in the average thaw depth along the two AL-transects closely resembled
540 the thaw depth observed using the ground temperature sensors in the sub-catchment. On the first day of sampling,
541 May 18th, 30% of the measurement points had a water level at or above the ground surface, and 7% of the points
542 were covered by surface water. The surface water formed several puddles, and two temporary surface streams that
543 crossed at least one of the AL-transects (Fig. 1). During the monitored period wet locations (with water table at
544 or above the ground surface) exhibited a higher thaw rate (0.8 cm day⁻¹) than dry locations (0.6 cm day⁻¹, p-value
545 <0.0001). The maximum observed thaw depth developed under one of the temporary surface streams, where the
546 thawed layer reached down to 48 cm below the ground surface on the last day of the monitoring period (May
547 31st).

548 **3.5 Stable water isotopes**

549 The stable water isotopic composition in temporary surface streams sampled in May 2017, as well as the average
550 for precipitation and lake water taken in 2011, 2014, 2017, and 2019, are shown in Fig. 5 and SI-Fig. 1. For the
551 precipitation there was a clear seasonality in the composition with more negative values in the snow samples
552 (average $\delta D = -159.7 \text{ ‰}$, standard deviation 12.5 ‰) compared to rain samples (average $\delta D = -115.8 \text{ ‰}$, standard

Deleted: precipitation

Deleted: or

Deleted: ,

Deleted: but

Deleted: most of the water

Deleted: sampling

Deleted: of

Moved (insertion) [1]

Deleted: studie

Deleted: d

Deleted: .The average thaw depth along the two AL-transects closely resembled the thaw depth observed using the ground temperature sensors in the sub-catchment, but there was

Moved up [1]: At the start of the intense monitoring period (May 18th) the average thaw depth along the studied transects was 10.4 cm, and by the end of the period (May 31st) it had increased to 15.3 cm.

Deleted: in ground thaw

Deleted: (Fig. 1)

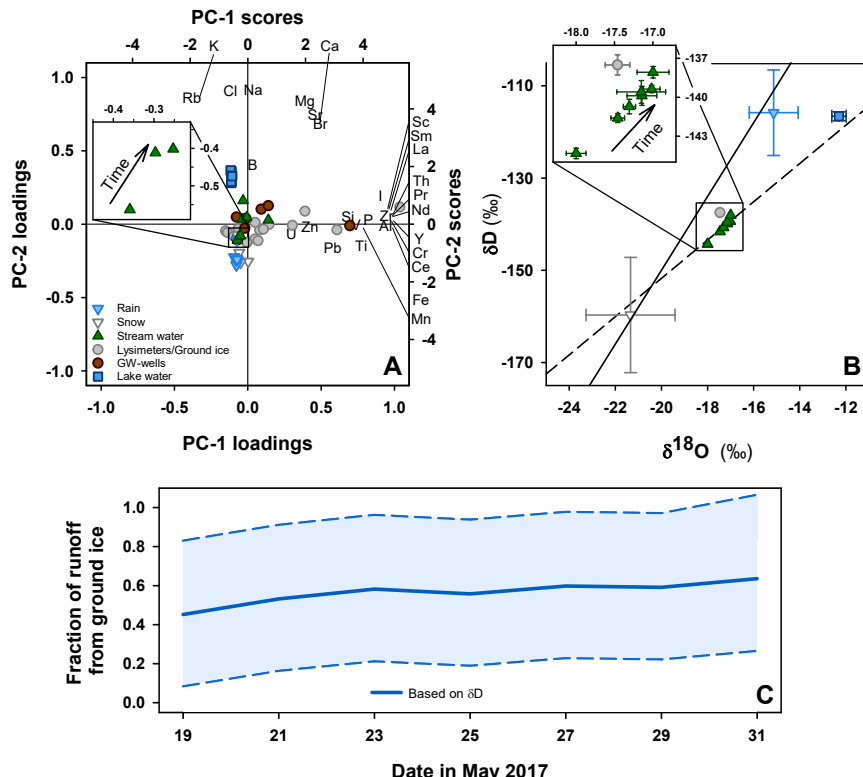
Deleted: occurred

Deleted: of water from

572 deviation 9.3 ‰). The compositions in samples from surface water (average $\delta D = -140.6$ ‰, standard deviation
 573 2.0 ‰) and ground ice (average $\delta D = -137.5$ ‰, standard deviation 0.8 ‰) showed a much smaller ~~variability~~,
 574 and the stable water isotopic values fell between the values for snow and rain (Fig. 5).

Deleted: spread

575



576
 577 Figure 5. Panel A consists of a combined loadings and score plot for the first two PCs (PC-1 and PC-2) ~~that gives~~ an
 578 overview of how the chemical signature varies between water types. Precipitation samples are found in the lower left-
 579 hand corner, while lake water samples are found in the upper left-hand corner. Surface water and soil water samples
 580 (lysimeter and groundwater wells) generally have similar or higher PC-1 scores compared to precipitation and lake
 581 water, with the highest scores found in soil water samples. For PC-2 surface and soil water are intermediate to
 582 precipitation and lake water samples. The insert shows the three water chemistry samples from the intense monitoring
 583 period, with the arrow indicating the trend with time. Panel B shows the average stable water isotopic composition (δD
 584 and $\delta^{18}\text{O}$) in snow, rain, ground ice samples, surface water and lake water samples. The symbols indicate the average,
 585 while the error bars indicate the standard deviation of all samples collected over the entire study period. The solid line
 586 represents the GMWL and the dashed line represents an evaporation line to indicate the trajectory of evaporating
 587 water. The insert shows the stable isotopic composition in the six surface water samples and the melted ground ice
 588 sampled in May 2017. The arrow indicates the trend with time, and error bars represent the variability between ~~field~~
 589 replicates. For access to the full datasets for both water chemistry and stable isotopic composition we refer to Lindborg
 590 et al. (2016) and its associated Pangaea databases (SI-Table 1). Panel C shows how the fraction of runoff from melting
 591

Deleted: ,

Deleted: intended to provide

594 ground ice and/or rain increases in the surface water over the intense monitoring period. The mixing model is based
595 on the change in δD in the temporary surface stream and using the average of rain (including ground ice) and snow as
596 endmembers.

597 During the two-week intense monitoring period the stable isotopic composition in samples from the temporary
598 surface streams changed considerably (Fig. 5). At the end of the monitoring period the δD signature of the surface
599 water was heavier and more closely resembled ground ice and rain than snow. The mixing model – which was
600 based on the δD in samples from temporary surface streams, rain (including ground ice), and snow – showed that
601 on the first day of sampling 39% of the surface water originated from rain, while 49% came from rain on the last
602 day of sampling (Fig. 5). The uncertainty range is high due to the high variability of values in samples of snow
603 and rain. Only 7 mm of rain fell during the intense monitoring period (and 3 mm the week before), while the
604 estimated release of water from melting of ground ice in the thawed part of the active layer was 18 mm. Most of
605 the released water therefore likely originated from rain that fell during the previous year and that had been stored
606 as ground ice during winter.

607 3.6 Surface water chemistry

608 The PCA identified five principal components (PCs) with eigenvalues above one, and together they explain 90%
609 of the variability in the data (Fig. 5). The first PC (PC-1) is driven by differences in elements related to silicate
610 minerals that can be assumed to be released through weathering (e.g., Al, Ce, Nd, La, Pr, Sc, Th, Y, Zr, P; Deer
611 et al., 1992). A part of the variability in Mg, Sr and Ca (i.e., elements also supplied via atmospheric deposition)
612 is also associated with this PC (the elements plot in the upper right-hand quadrant). Samples with high PC-1 scores
613 come from lysimeters and groundwater wells, i.e., water that has had more contact with soil particles, and samples
614 from precipitation and lake water have negative scores. DOC, which could not be included in the PCA because it
615 was not analysed in all of the samples used for ICP-MS analyses, showed a high positive correlation with PC-1
616 scores ($r_s=0.95$, p-value <0.001). The second PC (PC-2) is driven by elements that originate from the ocean (e.g.,
617 Cl and Na), and that are delivered to the catchment with precipitation. In addition, a part of the variability in
618 elements like Ca, Mg, Sr and K – which are all present in the precipitation but that could also be released during
619 interaction with soil particles – is associated with PC-2. For PC-2 there is a split between samples from the lake
620 on the positive side and precipitation on the negative side (with soil water samples in the middle). That the surface
621 and lake water have considerably higher concentrations of elements not released by weathering (e.g., Cl) as
622 compared to the precipitation indicates an enrichment caused by evapotranspiration (cf. Rydberg et al., 2023).
623 The remaining three PCs are driven primarily by a small number of samples without any obvious trends, and they
624 are therefore difficult to interpret in terms of processes. For the remainder of this paper, we will focus on PC-1
625 and PC-2, which both reflect processes that vary over the course of the year, e.g., depending on the source of the
626 water, the air temperature and the intensity in the runoff.

627 3.7 Correlations between hydrology and chemical signature of surface and soil water

628 During the intense monitoring period samples for geochemical analyses were collected on three occasions (May
629 19th, 25th and 31st). During this period the hydrological modelling suggests that the total runoff as both
630 groundwater and overland flow decreased (from 9.4 mm to 4.2 mm between May 19th and May 25th), and that it
631 then increased slightly to 6.0 mm on May 31st. During the same period the proportion of deep groundwater

Deleted: 1

Deleted: nce

Deleted: , which

Deleted: also are released through weathering.

Deleted: that

Deleted: po

Deleted: general

653 increased from 2.5 to 4.1 and finally 4.4% of the total runoff. Looking at the PC-scores, both PC-1 and PC-2
654 scores increased over the intense monitoring period. The PC-1 scores went from -0.36 on May 19th, to -0.30 and
655 then -0.25 on May 31st. For PC-2 the main shift occurred between the 19th and 25th when the score increased from
656 -0.56 to -0.41. On May 31st the PC-2 score was essentially the same as on May 25th (-0.40). During this period
657 DOC ~~decreased~~ from 20.8 mg L⁻¹ to 13.5 mg L⁻¹ and ~~then increased to~~ 14.7 mg L⁻¹.

Deleted: changed

Deleted: finally

658 If we look at surface-water samples collected in the studied sub-catchment during the entire 2011-2019 period
659 (n=7) the chemical signature in the surface water varies considerably. When the proportion of deep groundwater
660 is high, there is an increase in the concentration of weathering products released from soil particles (i.e., PC-1
661 scores). This results in a positive correlation between PC-1 and the proportion of deep groundwater ($r_s=0.79$,
662 $p=0.036$). For elements where the source is mainly precipitation and that are enriched through evapo~~transpiration~~
663 (i.e., PC-2), there is an increase in the concentrations as the total runoff decreases over the course of the unfrozen
664 season. For example, PC-2 scores are positively correlated with day-of-year (DOY; $r_s=0.89$, $p=0.007$), and there
665 is a negative correlation between PC-2 scores and total runoff ($r=-0.81$, $p=0.029$). For the surface-water samples
666 neither PC-1 nor PC-2 scores are correlated with DOC, but similar to PC-2 scores, DOC is negatively correlated
667 with the total runoff ($r=-0.59$, $p=0.017$).

Deleted: s

668 When looking at the lysimeters and groundwater wells – i.e., the soil water – a different pattern emerges. First,
669 the chemical signature in the soil water is even more variable compared to the surface water. Second, PC-1 and
670 PC-2 are correlated ($r_s=0.47$; $p=0.021$), and both are correlated with DOC ($r=0.92$, $p=0.001$ and $r=0.86$, $p=0.001$,
671 respectively). This indicates that even if the processes driving PC-1 (weathering), PC-2 (evapotranspiration) and
672 DOC (organic matter decomposition) are not related, there is a tendency that soil water is enriched in all three in
673 a similar way. In the soil water, DOC shows a negative correlation with total runoff ($r_s=-0.92$, $p<0.001$), while
674 neither PC-1 nor PC-2 scores for the soil water are correlated with any of the hydrological variables, and neither
675 PC-1, PC-2 nor DOC are correlated with sampling depth.

676 4 Discussion

677 4.1 Young water and shallow flow paths dominate runoff

Deleted: s the

678 The output from the extended hydrological modelling period (2013-2019) largely corroborates the findings from
679 the original modelling period (2011-2013; Johansson et al., 2015a). ~~In brief~~, Two-Boat Lake is situated in a dry
680 periglacial landscape, where a considerable fraction of the precipitation (55-80%) is lost through
681 ~~evapotranspiration in the terrestrial system (including sublimation)~~, and where surface water runoff is ~~almost~~
682 ~~exclusively~~ confined to high flow situations, ~~primarily~~ the snowmelt period. That there are ~~no~~ major differences
683 in the hydrological situation ~~between the two periods~~ is ~~consistent~~ with findings that the study area has not
684 experienced any significant change in climate over the period ~~from 2001 to 2019~~, even though a long-term (1981-
685 2019) warming trend has been suggested for the region (Hanna et al., 2021). All years except 2017, which was
686 slightly wetter (405 mm yr⁻¹) compared to the previously wettest year (i.e., 2012, 366 mm yr⁻¹), fall within the
687 range of 2011-2013 for precipitation, evapotranspiration and total runoff from the catchment to the lake (Fig. 2).
688 The annual pattern in runoff is also very similar. ~~Runoff is highest during the snowmelt period, which accounts~~
689 for about half of the annual runoff to the lake (Johansson et al., 2015a). During summer the total runoff decreases
690 as a response to increased evapotranspiration, ~~which generally exceeds the input of water during this period. When~~

Deleted: That is

Deleted: sublimation or

Deleted: mostly

Deleted: during

Deleted: t any

Deleted: in line

Deleted: study

Deleted: (

Deleted: -

Deleted:)

Deleted: ,

Deleted: (

Deleted: :

Deleted: . R

Deleted: (

710 evapotranspiration decreases in the fall (August-September) there is generally a slight increase in the total runoff
711 before the active layer freezes (Fig. 2).

Deleted:), while

Deleted: , evaporation decreases and

Deleted: to the lake increases again

Deleted: ground

Deleted: young (i.e.,

Deleted:)

712 According to our particle tracking simulation most of the groundwater that moves through the sub-catchment is
713 young, especially during the snowmelt period when almost all water in the saturated zone is less than 1-year old.
714 This is consistent with studies of water transit times in other permafrost areas using tracer methods (e.g. Cochand
715 et al., 2020; Tetzlaff et al., 2018; Throckmorton et al., 2016). Another interesting result of the particle tracking
716 simulation is that there is virtually no ground water in the active layer that is more than 10 years old. Again, this
717 is consistent with other studies in areas with continuous permafrost (Walvoord and Kurylyk, 2016). That a high
718 proportion of the water reaching a stream is young is common for all climate zones (Jasechko et al., 2016). For
719 example, in a similar particle tracking simulation, but made for a boreal forested catchment without permafrost,
720 most of the groundwater also was between 0.8- and 3.7-years old (Jutebring Sterte et al., 2021b). However, unlike
721 for the Two-Boat Lake catchment, where the maximum age of groundwater was a few years, a considerable
722 fraction (~25%) of the groundwater in the boreal system had an age of between 10 and 1000 years. This old
723 groundwater increases the average groundwater age substantially, and can explain that areas without permafrost
724 generally have older average groundwater ages compared to areas with continuous permafrost (Hiyama et al.,
725 2013; Wang et al., 2022). Older mobile groundwater can make an important contribution to surface waters also
726 in areas with continuous permafrost, but it requires the presence of through taliks that connect the deep
727 groundwater system below the permafrost with the surface system (Koch et al., 2024). Two-Boat Lake has such
728 a through talik, but the flow is directed downwards and there is no discharge of sub-permafrost groundwater in
729 the surface system (Johansson et al. 2015a). It should be noted that our model only simulates the age of
730 groundwater in the saturated zone, and that during the snowmelt period runoff occurs also as overland flow in the
731 temporary stream network. Therefore, our simulated water ages cannot be directly compared to results from tracer-
732 based methods.

Deleted: The simulation also suggests that old mobile groundwater (i.e., more than 10 years) is lacking in Two-Boat Lake, which is in line with other studies from supra-permafrost groundwater systems in areas with continuous permafrost (Walvoord and Kurylyk, 2016). The results of our particle tracking simulation also align with studies of water transit times in permafrost areas using tracer methods, indicating that it is common that most of the water that moves through permafrost landscapes is young (e.g. Cochand et al., 2020; Tetzlaff et al., 2018; Throckmorton et al., 2016).

Deleted: However, a

Deleted: water

Deleted: common

Deleted: in streams

Deleted: in

Deleted: , but in continuous permafrost landscapes water ages are even lower than in areas without permafrost (Hiyama et al., 2013; Wang et al., 2022). For example,

Deleted: indicated that

Deleted: .

Deleted: be

Deleted: present

Deleted: , e.g., because of a connection to the groundwater system below the permafrost through taliks

Deleted: Th

Deleted: at this effect cannot be seen in Two-Boat Lake

Deleted: is likely related to the recharging nature of the talik under Two-Boat Lake

733 Even if the groundwater in Two-Boat Lake generally is young, there is a clear seasonal trend with increasing
734 water age as the unfrozen season progresses. This pattern can be seen in the 0-25 cm layer, but it is especially
735 pronounced in the 25-50 cm layer. At the deepest layer, i.e., 50-75 cm, there is no clear seasonal trend, but most
736 of the water that moves in this layer is older than two years. These patterns imply several things. First, the
737 movement of water in the uppermost layer (i.e., 0-25 cm) is mostly restricted to the snowmelt period, and as the
738 thaw depth increases, the groundwater takes deeper flow paths. Similar patterns have been documented from other
739 permafrost regions (Juhls et al., 2020; Lebedeva, 2019; Zastruzny et al., 2024). Second, the turnover time of the
740 water in the uppermost layer is short, but the time that the water has spent in contact with the soil particles
741 increases as the unfrozen season progresses. Third, for the deepest analysed layer (i.e., 50-75 cm) the turnover
742 time is longer, and most of the water has spent several seasons in contact with the soil particles and undergone at
743 least one freeze-thaw cycle.

Deleted: s

Deleted: relatively

Deleted: the saturated zone, i.e., this water has

744 4.2 The effects of fast and shallow flow paths on the water chemistry

745 Most of the variability in water chemistry can be explained by either the amount of weathering products (PC-1)
746 that have been released from soil particles or the degree of evaporative loss the water has experienced (PC-2).
747 Because the PC-1 and PC-2 scores for the surface-water samples are correlated to different hydrological variables
748 from the hydrological modelling it seems as if these two components are influenced by separate processes. For

Deleted: accumulated

Deleted: through interactions with

Deleted: based on the correlations between

Deleted: for the surface-water samples and the

Deleted: controlled

Deleted: hydrological factors

791 surface water, PC-2 scores – which represent elements supplied with precipitation and that are concentrated
792 through evapotranspiration – show a negative correlation with total runoff. In spring, when large volumes of
793 snowmelt water move through the system, the chemical signature is more diluted and closer to that of
794 precipitation. The PC-2 scores then progressively increase over the unfrozen season, and the chemical signature
795 of the surface water shifts towards a signature that is more characteristic of the lake water (Fig. 5). This implies
796 that as the water from precipitation moves through the catchment and is exposed to evapotranspiration, it becomes
797 more concentrated in elements that were present in the precipitation when it was deposited (e.g., chlorine, Cl).
798 This interpretation is also consistent with the PC-2 scores being positively correlated with DOY, and with water
799 ages increasing as the unfrozen season progresses (Fig. 3). That evapotranspiration is an important process in this
800 dry landscape can also be seen in the hydrological model, where two-thirds to four-fifths of the annual
801 precipitation leaves the terrestrial system as sublimation or evapotranspiration. This loss of water translates to a
802 concentration factor of 3-5, which is consistent with the 3.3 times increase in Cl concentration between
803 precipitation and surface water (SI-Table 2). Chlorine is almost exclusively supplied via precipitation and is often
804 used as a conservative tracer for the input of solutes via precipitation (Johnson et al., 2000; Lockwood et al.,
805 1995).

806 For elements supplied through weathering it is not ~~the~~ the amount of runoff that is of importance. Instead, it is the
807 proportion of runoff classified as deep groundwater (i.e., 50-75 cm depth in our model) that ~~is correlated to the~~
808 ~~PC-1 scores~~. In July and August, when the proportion of deep groundwater in the runoff is high, the particle
809 tracking suggests that the majority of the ~~the~~ groundwater has spent more than two years in the saturated zone (Fig.
810 3). From the soil-water samples we can see that this older water ~~is~~ rich in weathering products (i.e., high PC-1
811 scores, Fig. 5), something that ~~has also been shown in~~ studies in other systems and other regions (Jutebring Sterte
812 et al., 2021b; Williams et al., 2015). When looking at the concentrations ~~of~~ calcium (Ca, supplied both via
813 precipitation and weathering), lanthanum (La; supplied primarily via weathering) and Cl in ~~samples from~~ precipitation and surface water they show different enrichment patterns (Deer et al., 1992; Johnson et al., 2000).
814 As mentioned above, Cl increases about 3.3 times between precipitation and surface water, and the enrichment
815 can therefore be explained by evapotranspiration alone. For La and Ca the difference is higher, 7.8 and 10 times,
816 respectively (SI-Table 2), which indicates that these elements must also be supplied by an internal process in the
817 catchment (e.g., weathering). This interpretation is also in line with the mass-balance budget that Rydberg et al.
818 (2023) developed for Two-Boat Lake, ~~which~~ suggests that La is exclusively supplied by weathering, Cl almost
819 exclusively via precipitation and Ca is supplied by both processes.

820 Even if DOC was not measured on all sampling occasions, and could not be included in the PCA, the correlation
821 between PC-1, PC-2 and DOC helped us to assess if organic carbon behaves like weathering products or elements
822 supplied with precipitation. For the surface-water samples there is no correlation between PC-1, PC-2 and DOC,
823 but similarly to PC-2, DOC is negatively correlated with the total runoff. The different behaviours of weathering
824 products (PC-1) and DOC could be related to where in the soil profile these products originate. DOC production
825 is highest in ~~the~~ uppermost soil layer, where the decomposition of relatively fresh OM is highest (Clark et al.,
826 2008). These surficial layers thaw relatively rapidly, and hence, the DOC source is activated already during the
827 snowmelt period. This means that, like the elements represented by PC-2, DOC is diluted when the runoff is high.
828 However, unlike the elements that are constantly resupplied with the precipitation, DOC in the upper soil layers
829 can become depleted with time, and PC-2 and DOC are therefore not correlated (Stewart et al., 2022). Weathering

Deleted: at is,

Deleted: fell

Deleted: , Cl

Deleted: 1

Deleted: primarily

Deleted: has an effect

Deleted: is deep

Deleted: d

Deleted: T

Deleted: at

Deleted: and deeper ground

Deleted: is

Deleted: er

Deleted: is

Deleted: consistent with

Deleted: in

Deleted: 1

Deleted: soils

Deleted: i.

Deleted: and

Deleted: s

852 products on the other hand are primarily produced deeper in the soil profile (Cai et al., 2008; Fouché et al., 2021),
853 and it is not until later in the season when these deeper layers thaw ~~that~~ the proportion of deep groundwater in the
854 runoff increases. A similar shift in the chemical composition when the thaw in the active layer reaches below the
855 upper organic-rich soil layer, has been observed in other areas with continuous permafrost (Cai et al., 2008;
856 Chiasson-Poirier et al., 2020).

Deleted: – and

Deleted: – that this source becomes activated

857 Looking at the soil water ~~from~~ lysimeters and ~~groundwater wells~~, PC-1, PC-2 and DOC are all correlated, which
858 ~~would~~ indicate that ~~the soil~~ water is enriched in both weathering products, elements supplied with precipitation
859 and DOC. One explanation for this is that a high DOC concentration can also lead to a higher solubility of many
860 elements, particularly weathering products that otherwise can have a low solubility in water (Broder and Biester,
861 2015; Lidman et al., 2017). That ~~soil and groundwater~~ is enriched in ~~many~~ elements is also consistent with
862 previous studies that have shown that deeper and older groundwater often has elevated concentrations for a large
863 selection of elements (Clark et al., 2008; Fouché et al., 2021; Stewart et al., 2022). Unlike previous studies in
864 Greenland (Jessen et al., 2014), neither PC-1, PC-2 or DOC showed any correlation with sampling depth. ~~This~~
865 ~~likely~~ has several reasons. First, the depths where the lysimeters are installed (15, 30 ~~and~~, 35 cm) correspond to
866 the two upper layers used in the particle tracking simulation (i.e., 0-25 and 25-50 cm). In these two layers the age
867 of the water is relatively similar, and it is possible that a clearer pattern would have emerged if the deepest
868 lysimeter had been placed in the ~~50-75-cm~~ layer used in the particle tracking simulation where the water is
869 considerably older. Second, ~~because they are frozen longer~~ the deeper lysimeters could only be sampled late in
870 the season when the total runoff was low. The lack of trend with depth could therefore also be a result of this bias
871 in the data. Third, the generally similar age for the two upper layers in the particle tracking simulation suggests
872 that there is a considerable vertical movement of water in the ~~upper part of the~~ thin unfrozen layer. ~~This results in~~
873 mixing of the water ~~and~~ would prevent the development of a consistent vertical trend in the chemical ~~signature of~~
874 ~~the water.~~

Deleted: sampled using

Deleted: in

Deleted: c

Deleted: older, and deeper,

Deleted: ground

Deleted: ground

Deleted: , which

Deleted: and

Deleted: /

Deleted: deepest

Deleted: (i.e., 50-75 cm)

Deleted: because they are frozen during the entire snowmelt period...

Deleted: that results

Deleted: . This mixing

Deleted: ny

Deleted: composition

876 4.3 Variability in thaw rates during snowmelt on different timescales

877 Similar to the original modelling period (Johansson et al., 2015a), the runoff ~~during the entire 2011-2019 period~~
878 ~~was~~ dominated by groundwater, either directly to the lake or via temporary surface streams. ~~The addition of the~~
879 extended modelling period ~~did, however, reveal~~ ~~much~~ more between-year variability. Even though the annual
880 precipitation ~~was~~ relatively similar between 2014, 2015, 2016 and 2018 (247, 284, 286 and 261 mm yr⁻¹,
881 respectively) the amount of overland flow varied considerably. 2014 and 2015 had a very low contribution of
882 overland flow (less than 15% of total runoff), whereas in 2016 and 2018 around 50% of the annual runoff occurred
883 as overland flow either directly to the lake or via temporary surface streams. These differences in the partitioning
884 between groundwater and overland flow from one year to the other can likely be linked to ~~a combination of~~ the
885 amount of accumulated snow in the catchment, ~~the timing of the snowmelt period and the hydrological conditions~~
886 ~~during the preceding year. In the winters preceding the snowmelt periods of 2014 and 2015 the amount of winter~~
887 precipitation (October to March) ~~was~~ relatively close to the average (105 and 155 mm, respectively) and the
888 snowmelt ~~period~~ started relatively late (mid to late May), ~~indicating a rapid thaw in the active layer due to higher~~
889 ~~temperatures and longer days.~~ This resulted in a low proportion of the runoff leaving as overland flow during
890 these years. In 2016, considerably more snow fell during the preceding winter (220 mm) and the snowmelt started

Deleted: by

Deleted: (

Deleted: i

Deleted: ,

Deleted: , but the

Deleted:

Deleted: s

Deleted: i

Deleted: s

Deleted: ve

Deleted: both

Deleted: and

Deleted: haw r

Deleted: ate in the active layer, especially early in the thaw season.

Deleted: T

Deleted: , which dominantly fell as snow

Deleted: during the winters preceding the snowmelt periods of 2014 and 2015 ...

928 already in early April. Together this resulted in a higher proportion of the annual runoff leaving the catchment as
929 overland flow. For 2018, the amount of accumulated snow was low (91 mm) and the snowmelt period started in
930 mid-May, i.e., similarly to 2014 and 2015. Still, during 2018 a much larger percentage of the annual runoff left
931 the terrestrial catchment as overland flow (52%) compared to during 2014 and 2015. This can most likely be
932 attributed to the preceding year, 2017, which was considerably wetter compared to all other years (407 mm yr⁻¹
933 of annual precipitation). This resulted in a high soil moisture content and high groundwater levels when the active
934 layer froze in the autumn of 2017. A high content of ground ice in the active layer implies that the capacity for
935 infiltration during the snowmelt period was limited, and the latent heat content in the ice likely contributed to a
936 slower thaw rate in the active layer in 2018 compared to other years (Clayton et al., 2021). As the ground surface
937 thawed, the high soil moisture content may also have contributed to saturation-excess overland flow occurring
938 during the late snowmelt and summer periods. For all other years, overland flow did not occur during summer,
939 presumably because the generally dry conditions normally result in most water infiltrating the ground surface
940 during summer. For example, observations in the field confirm that temporary surface streams normally only
941 appear during limited periods during the snowmelt period and wet periods during fall.
942 While the long-term hydrological modelling indicated that interannual variability in thaw in the active layer can
943 have an influence on runoff patterns, our field observations during the intense monitoring period revealed that –
944 on a finer spatial scale – the hydrology also controls thaw rates. The thaw-depth monitoring during May 2017
945 showed that wet locations thawed significantly faster than drier locations. This would support earlier findings
946 from areas with continuous permafrost, where variability in the active layer thickness has been attributed to the
947 development of a hillslope groundwater drainage system (Chiasson-Poirier et al., 2020). The fastest thaw rates
948 and largest thaw depths in the Two-Boat Lake catchment were measured in wet locations and directly under the
949 temporary surface streams. This would suggest that advective heat transport with surface water and near-surface
950 groundwater plays an important role in determining the thaw rate, as has been observed elsewhere in the Arctic
951 (Dagenais et al., 2020; De Grandpré et al., 2012; Sjöberg et al., 2016). When compared to earlier investigations
952 in the Two-Boat Lake catchment, it is noticeable that the maximum measured thaw depth during the intense
953 monitoring period (48 cm on May 31st), was almost the same as the average active layer thickness observed for
954 the same vegetation type (i.e., wetland) in August 2011 (Petrone et al., 2016). This indicates that the ground in
955 connection to temporary surface streams thaws rapidly during the snowmelt period, but that the rate of thaw is
956 much slower during the remainder of the summer season. At the drier location where the ground temperatures are
957 monitored down to 2-m depth the thaw developed slower. In 2017 the 50-cm and 75-cm sensors reached
958 temperatures above zero on June 9th and July 27th respectively (i.e., considerably later than under the temporary
959 stream). Taken together with the drier locations having deeper maximum thaw depths compared to wetlands (70–
960 80 cm; Petrone et al., 2016), this indicates that even if wetter locations thaw more rapidly in spring due to advective
961 heat transfer, the effect of the latent heat in wet soils becomes more important in determining the maximum thaw
962 depth later in the season.
963 This fine-scale variability in thaw rates in the active layer was not included in our hydrological modelling and
964 subsequent particle tracking simulation. The finding that the thaw rate is faster under the temporary stream
965 network means that deeper soil layers are activated earlier than expected from the ground temperature loggers
966 used by the model simulation. This suggests that water that reaches the lake during the snowmelt period may be

Deleted: which

Deleted: slightly

Deleted: er

Deleted: water

Deleted: (7 and 13%, respectively)

Deleted: being

Deleted: at the time

Deleted: this year

Deleted: (evapotranspiration exceeds precipitation)

Deleted: high

Deleted: on

Deleted: during

Deleted: exerts a strong control on

Deleted: the

Deleted: of the slope

Deleted: ±9 cm

Deleted: under

Formatted: Superscript

Deleted: similar

Deleted: cover

Deleted: by

Deleted: (

Deleted: reported

Deleted: temperatures

Deleted: the 75-cm sensor on

Deleted: .

Deleted: (Clayton et al., 2021).

Deleted: suggests

Deleted:

995 more affected by the interaction with soil particles and pre-event water than our modelling indicates. It also
996 suggests that our simulated groundwater ages may be an underestimate of water age early in the season.▼

997 4.4 The influence of melting ground ice on the chemical composition during the snowmelt period

998 Looking at the isotopic composition of the surface water samples from the Two-Boat Lake catchment, they are
999 heavier for both the hydrogen (δD) and oxygen ($\delta^{18}\text{O}$) than surface waters from Pituffik in northern Greenland
000 (Akers et al., 2024), the Scotty Creek drainage system in Canada (Hayashi et al., 2004), and surface waters from
001 the Yukon region of Canada and Alaska (Lachniet et al., 2016; SI-Fig.1). This heavier signal is likely related to
002 dominant wind patterns and relatively warm sea surface temperatures in the source area for the water that falls as
003 rain and snow on the Two-Boat Lake catchment (Sodemann et al., 2008; SI-Fig. 1). For the stable isotopic
004 composition in stream samples collected during the intense monitoring period there is a temporal trend that
005 roughly follows the evaporation line (Fig. 5B). On the one hand, this could suggest fractionation during
006 evapotranspiration, sublimation, condensation, and freezing-thawing processes. On the other hand, there is a
007 deviation away from the evaporation line toward the composition of rain and ground ice during the end of the
008 intense monitoring period (Fig. 5B). This suggest that the deviation is driven by an increased influence of water
009 from melting ground ice as the thaw depth increases over the monitoring period. This would be consistent with
010 the mixing model, which suggests a larger contribution of water from rain and ground ice at the end of the
011 monitoring period (Fig. 5C).▼

012 Ground ice that fills the pore spaces in the active layer (i.e., non-segregated ground ice) most likely formed from
013 the water present in the active layer the previous fall when the ground froze (although some infiltration and
014 migration of meltwater during warm periods in winter cannot be completely excluded). According to the particle
015 tracking simulation, most water that was present in the active layer during the fall freeze-up is at least one year
016 old, and a substantial fraction is older than four years. This implies that the ground ice consists of a mixture of
017 water from summer and winter precipitation, which can explain that the stable isotopic composition of ground ice
018 falls between snow and rain (Fig. 5B). That the groundwater carries an isotopic signal from summer and winter
019 precipitation is consistent with observations in the continuous permafrost zone in northern Canada (Tetzlaff et al.,
020 2018, Wilcox et al., 2022), whereas, findings in lowland polygonal tundra in the continuous permafrost zone in
021 Alaska indicate that winter precipitation did not contribute to the stable isotopic signature of active layer pore
022 waters (Throckmorton et al., 2016).

023 Similar to the stable isotopic signature, there was a shift in the chemical signature during the intense monitoring
024 period. PC-1 increased, PC-2 first increased and then remained stable, while DOC first decreased and then
025 increased slightly. The increase in PC-1 is consistent with patterns observed over the entire unfrozen period, i.e.,
026 PC-1 increase when the proportion of deep groundwater in the runoff increase. For PC-2 there is an increase from
027 May 19th to May 25th when the total runoff decreases, which is consistent with the entire unfrozen period (Fig.
028 5A). However, when the total runoff then increases again to May 31st, the PC-2 scores remain virtually unchanged.
029 The DOC decreases when the total runoff decreases from May 19th to May 25th, and it then increases slightly until
030 May 31st. This suggests that the chemical signature is not merely a question of more or less water, we also need
031 to consider where the water comes from. From the stable isotopic signature of the ground ice, we can see that
032 there is a considerable influence of melting ground ice over the intense monitoring period. The water from this
033 melting ground ice will not only be isotopically heavier (δD and $\delta^{18}\text{O}$) compared to the meltwater from snow, this

Deleted: in...nteraction more ...ith soil particles and pre-event water than what ...ur modelling indicates. It also suggests that ...O...r simulated groundwater ages may also ...e an underestimate of of the...content of older ...ater age earlyier...in the season. , as considerably deeper soil layers are thawed earlier in the season and possibly in a connected drainage pattern, similar to that observed by Chiasson-Poirier (2020) in northern Canada. □ [1]

Deleted: were roughly 5 %

Formatted: Superscript

Deleted: in...the Yukon region of Canada and Alaska (Lachniet et al., 2016)... SI-Fig.1). This heavier signal is likely related to wind patterns and relatively warm sea surface temperatures in the source area for the water ...hat falls as rain and snow on the Two-Boat Lake catchment (Sodemann et al., 2008; SI-Fig. 1). For the stable isotopic composition in stream samples collected during the intense monitoring period there is a temporal trend that roughly follows the evaporation line (Fig. 5B). On the one hand, tT...is could suggest fractionation during evapotranspiration, sublimation, condensation, and/or freezing-thawing processes. On the other hand, , but because □ [2]

Moved (insertion) [2]

Deleted: at the end of the monitoring period...his is directed toward the composition of rain and ground ice ...suggest that the deviation is driven by an increased influence of water from melting ground ice as the thaw depth increases over the monitoring period. it could also be related to a shift in the source of the stream water □ [3]

Moved up [2]: (Fig. 5B).

Deleted: An influence of melting ground ice ...his would be consistent with the mixing model, which suggests a larger contribution of water from rain and ground ice at the end of the monitoring period (Fig. 5C), mixing model (Fig. 5C), which suggests that the isotopic signature of the stream water is heavily influenced by melting ground ice. □ [4]

Deleted: G...ound ice that fills...the pore spaces in the active layer (i.e., non-segregated ground ice) most likely formed from the water present in the active layer during ...he previous fall when the ground froze (, ...lthough some infiltration and migration of meltwater during warm periods during the...n winter cannot be completely excluded). According to the particle tracking simulation, most water that was present in the active layer during the fall freeze-up is at least one year older than four years. This implies that the ground ice consists of a mixture of water from summer and winter precipitation, which can explain that . In light of this, ...he stable isotopic composition of the ground ice falls...somewhere in the middle ...tween those of snow and rain (Fig. 5B) ... That the groundwater carries an isotopic signal from summer and winter precipitation is consistent to be expected and has al...th so been ...bservations found using similar methods ...n the continuous permafrost zone in northern Canada (Tetzlaff et al., 2018, Wilcox et al., 2022), whereas . In comparison to findings in lowland polygonal tundra in the continuous permafrost zone in Alaska indicate , where ...hat winter precipitation did not contribute to the stable isotopic signature of active layer pore waters , water in the active layer in Two-Boat Lake appears to be more well mixed at least in the fall □ [5]

Deleted: ... a shift in the chemical signature during the intense monitoring...period. PC-1 increased, PC-2 first increased and then remained stable, and ...hile DOC first decreased and then increased slightly. The increase in PC-1 is consistent with patterns observed over the entire unfrozen period, i.e., PC-1 and it ...ncrease s ...hen as the proportion of deep groundwater in the runoff increases... For PC-PC-2 and DOC, the trends during the intense monitoring period do not show the same negative correlation with total runoff as during the entire unfrozen season. ...or PC-2 there is an initial ...ncrease from May 19th to May 25th...when the total runoff decreases, which is consistent with the expected ...ntire unfrozen period trend... (Fig. 5A). However, when the total runoff then increases again to May 31st, the PC-2 scores remain virtually the same...nchanged as on May 25th... The DOC decreases when the total runoff decreases from May 19th to May 25th, and it then increases slightly until May 31st. □ [6]

264 pre-event water will also be enriched in elements related to both PC-1, PC-2 and have a higher DOC concentration.
265 That thaw of ground ice and permafrost has a profound effect on the chemical signature of soil water in permafrost
266 regions has also been reported from sites in Alaska (Fouché et al., 2021), and the importance of pre-event water
267 have been shown for a wide variety of environmental settings (Fischer et al., 2017; Juhls et al., 2020; Ross et al.,
268 2017). Furthermore, presumably most of the water from melted ground ice comes from the near stream zone,
269 where the thaw rate is highest. This suggests that these temporary “riparian” zones are important for the evolution
270 of the stable isotopic and chemical signature of the surface water, which is analogous to the importance of the
271 riparian zone in other systems (Jutebring Sterte et al., 2022; Lidman et al., 2017).

1272 Conclusions

273 Our field measurements of thaw rates in the active layer during the 2017 snowmelt period shows that, even if drier
274 areas tend to have a thicker active layer in August (Petrone et al. 2016), areas in connection with temporary surface
275 streams thaw more rapidly early in the unfrozen season. The rapid formation of an unfrozen zone beneath these
276 temporary streams allows meltwater to interact with soil particles and pre-event water already early in the
277 snowmelt period. This is reflected in, e.g., the stable isotopic signature of stream water, which initially resembles
278 that of snow but quickly shifts toward a signature more similar to melting ground ice that consists of a mixture of
279 rain and snow from previous seasons.

280 Based on the hydrological modelling, we can also conclude that although interannual differences in the
281 hydrological conditions can result in up to half of the runoff occurring as overland flow in some years, runoff to
282 Two-Boat Lake is generally dominated by groundwater. Even if most of this groundwater is less than one year,
283 the particle tracking simulation shows that a considerable fraction of the water in deeper soil layers (i.e., 50-75
284 cm) is older than three years. The proportion of this old and “deep” groundwater is an important factor for
285 controlling the chemical signature of the water entering Two-Boat Lake, especially for elements released through
286 weathering. However, although the interaction between the runoff and soil particles is important, it is not the only
287 process influencing the chemical signature of the runoff. For elements supplied via precipitation, our data suggest
288 that in this dry landscape, evapotranspiration also has a strong influence on the concentrations of elements in the
289 runoff.

290 Taken together, this indicates that even if runoff is dominated by the snowmelt period, groundwater generally is
291 young, and continuous permafrost restricts water movement to the thin active layer, there is a strong connection
292 between terrestrial processes and the chemical signature of the runoff. This connection is especially important
293 when considering the substantial variability in both hydrological conditions and thaw rates—both spatially and
294 temporally—and it highlights the importance of accounting for the effect of soil processes and mixing with pre-
295 event water when assessing water quality and element transport in Arctic landscapes with continuous permafrost.

296
297 **Data availability**
298 The data used in this study is available mainly through three publications, Johansson et al. (2015b), Lindborg et
299 al. (2016) and Petrone et al. (2016), each with an adjoined Pangaea dataset. For Johansson et al. (2015b) and
300 Lindborg et al. (2016) data covering the period up to August 2019 are available through two additional Pangaea
301 datasets that are linked to the original publications. Meteorological data from the automated weather station

Deleted: that has resided in the ground for an extended time
Deleted: has higher
Deleted: s
Deleted: 1
Deleted: the thaw of
Deleted: at
Deleted: and elements that can be flushed from surficial soil layers
Deleted: to be important also under

Deleted: monitoring
Deleted: by
Deleted: in the
Deleted: stages

Deleted: .

Deleted: The particle tracking simulation shows that
Deleted: while
Deleted: young-i.e.,
Deleted: –indicating limited interaction with soil particles
Deleted: This
Deleted: plays an important role for
Deleted: in
Deleted: runoff to
Deleted: 1
Deleted: ,
Deleted: that
Deleted: extensive evapotranspiration
Deleted: ly affects
Deleted: the
Deleted: the
Deleted: the
Deleted: remains
Deleted:
Deleted: 1
Deleted: 1
Deleted: base (doi:10.1594/PANGAEA.845258, doi:10.1594/PANGAEA.860961 and doi:pangaea.de/10.1594/PANGAEA.836178, respectively)
Deleted: additional
Deleted: has been made public
Deleted: databases

341 (labelled KAN_B) is available via www.promice.org. A summary of the different datasets and how to access them
342 can be found in SI-Table 1.

1343 **Author contribution**

1344 **JR**: Conceptualization, Formal analysis, Investigation, Writing – Original draft, **EL**: Conceptualization,
1345 Methodology, Formal analysis, Writing – Review & Editing, **CB**: Formal analysis, Writing – Review & Editing,
1346 **BMCF**: Writing – Review & Editing, **TL**: Conceptualization, Investigation, Writing – Review & Editing, **YS**:
1347 Conceptualization, Formal analysis, Investigation, Writing – Original draft.

1348 **Competing interests**

1349 Ylva Sjöberg is a member of the editorial board of The Cryosphere

1350 **Acknowledgement**

1351 This study was funded by Swedish nuclear fuel and waste management company (SKB) within the Greenland
1352 Analogue Surface Project (GRASP) and CatchNet project. We also thank two anonymous reviewers for valuable
1353 input during the review process.

1354 **References**

1355 Akers, P. D., Kopec, B. G., Klein, E. S., Bailey, H., and Welker, J. M.: The Pivotal Role of Evaporation in Lake
1356 Water Isotopic Variability Across Space and Time in a High Arctic Periglacial Landscape, *Water
1357 Resources Research*, 60, e2023WR036121, <https://doi.org/10.1029/2023WR036121>, 2024.
1358 Alvarez, M. D., Carol, E., and Dapeña, C.: The role of evapotranspiration in the groundwater hydrochemistry of
1359 an arid coastal wetland (Peninsula Valdes, Argentina), *Science of the Total Environment*, 506, 299-307,
1360 10.1016/j.scitotenv.2014.11.028, 2015.
1361 Böcher, T. W.: Climate, soil, and lakes in continental West Greenland in relation to plant life, 1949.
1362 Bosson, E., Selroos, J. O., Stigsson, M., Gustafsson, L. G., and Destouni, G.: Exchange and pathways of deep and
1363 shallow groundwater in different climate and permafrost conditions using the Forsmark site, Sweden, as
1364 an example catchment, *Hydrogeology Journal*, 21, 225-237, 10.1007/s10040-012-0906-7, 2013.
1365 Bring, A., Fedorova, I., Dibike, Y., Hinzman, L., Mård, J., Mernild, S. H., Prowse, T., Semenova, O., Stuefer, S.
1366 L., and Woo, M. K.: Arctic terrestrial hydrology: A synthesis of processes, regional effects, and research
1367 challenges, *Journal of Geophysical Research-Biogeosciences*, 121, 621-649, 10.1002/2015jg003131,
1368 2016.
1369 Broder, T. and Bieser, H.: Hydrologic controls on DOC, As and Pb export from a polluted peatland – the
1370 importance of heavy rain events, antecedent moisture conditions and hydrological connectivity,
1371 *Biogeosciences*, 12, 4651-4664, doi:10.5194/bg-12-4651-2015, 2015.
1372 Bush, R. T., Berke, M. A., and Jacobson, A. D.: Plant Water δ D and δ 18O of Tundra Species from West
1373 Greenland, Arctic, Antarctic, and Alpine Research, 49, 341-358, 10.1657/AAAR0016-025, 2017.
1374 Cai, Y. H., Guo, L. D., and Douglas, T. A.: Temporal variations in organic carbon species and fluxes from the
1375 Chena River, Alaska, *Limnology and Oceanography*, 53, 1408-1419, 10.4319/lo.2008.53.4.1408, 2008.
1376 Chiasson-Poirier, G., Franssen, J., Lafrenière, M. J., Fortier, D., and Lamoureux, S. F.: Seasonal evolution of active
1377 layer thaw depth and hillslope-stream connectivity in a permafrost watershed, *Water Resources Research*,
1378 56, 10.1029/2019wr025828, 2020.
1379 Claesson Liljedahl, L., Kontula, A., Harper, J., Näslund, J. O., Selroos, J.-O., Pitkänen, P., Puigdomenech, I.,
1380 Hobbs, M., Follin, S., Hirschorn, S., Jansson, P., Kennell, L., Marcos, N., Rskenniemi, T., Tullborg, E.-L.,
1381 and Vidstrand, P.: The Greenland Analouge Project: Final Report, SKB, StockholmTR-14-13, 2016.
1382 Clarhäll, A.: SKB studies of the periglacial environment – report from field studies in Kangerlussuaq, Greenland
1383 2008 and 2010, Swedish Nuclear Fuel and Waste Management CoP-11-05, 2011.

1384 Clark, J. M., Lane, S. N., Chapman, P. J., and Adamson, J. K.: Link between DOC in near surface peat and stream
 1385 water in an upland catchment, *Science of the Total Environment*, 404, 308-315,
 1386 10.1016/j.scitotenv.2007.11.002, 2008.

1387 Clayton, L. K., Schaefer, K., Battaglia, M. J., Bourgeau-Chavez, L., Chen, J., Chen, R. H., Chen, A., Bakian-
 1388 Dogaheh, K., Grelit, S., Jafarov, E., Liu, L., Michaelides, R. J., Moghaddam, M., Parsekian, A. D., Rocha,
 1389 A. V., Schaefer, S. R., Sullivan, T., Tabatabaeenejad, A., Wang, K., Wilson, C. J., Zebker, H. A., Zhang,
 1390 T., and Zhao, Y.: Active layer thickness as a function of soil water content, *Environmental Research
 Letters*, 16, 055028, 10.1088/1748-9326/abfa4c, 2021.

1391 Cochand, M., Molson, J., Barth, J. A. C., van Geldern, R., Lemieux, J. M., Fortier, R., and Therrien, R.: Rapid
 1392 groundwater recharge dynamics determined from hydrogeochemical and isotope data in a small permafrost
 1393 watershed near Umiujaq (Nunavik, Canada), *Hydrogeology Journal*, 28, 853-868, 10.1007/s10040-020-
 1394 02109-x, 2020.

1395 Condon, L. E., Markovich, K. H., Kelleher, C. A., McDonnell, J. J., Ferguson, G., and McIntosh, J. C.: Where Is
 1396 the Bottom of a Watershed?, *Water Resources Research*, 56, 10.1029/2019wr026010, 2020.

1397 Dagenais, S., Molson, J., Lemieux, J. M., Fortier, R., and Therrien, R.: Coupled cryo-hydrogeological modelling
 1398 of permafrost dynamics near Umiujaq (Nunavik, Canada), *Hydrogeology Journal*, 28, 887-904,
 1399 10.1007/s10040-020-02111-3, 2020.

1400 de Grandpré, I., Fortier, D., and Stephani, E.: Degradation of permafrost beneath a road embankment enhanced
 1401 by heat advected in groundwater, *Canadian Journal of Earth Sciences*, 49, 953-962, 10.1139/e2012-018,
 1402 2012.

1403 Deer, W. A., Howie, R. A., and Zussman, J.: An introduction to the rock-forming minerals, 2nd, Longman
 1404 Scientific & Technical, Harlow 1992.

1405 EU: Guidance on Monitoring for the Water Framework Directive, 2002.

1406 Fischer, B. M. C., Stähli, M., and Seibert, J.: Pre-event water contributions to runoff events of different magnitude
 1407 in pre-alpine headwaters, *Hydrology Research*, 48, 28-47, 10.2166/nh.2016.176, 2017.

1408 Fischer, B. M. C., Rinderer, M., Schneider, P., Ewen, T., and Seibert, J.: Contributing sources to baseflow in pre-
 1409 alpine headwaters using spatial snapshot sampling, *Hydrol. Process.*, 29, 5321-5336, 10.1002/hyp.10529,
 1410 2015.

1411 Fouché, J., Bouchez, C., Keller, C., Allard, M., and Ambrosi, J. P.: Seasonal cryogenic processes control supra-
 1412 permafrost pore water chemistry in two contrasting Cryosols, *Geoderma*, 401,
 1413 10.1016/j.geoderma.2021.115302, 2021.

1414 Frey, K. E. and McClelland, J. W.: Impacts of permafrost degradation on arctic river biogeochemistry, *Hydrol.
 1415 Process.*, 23, 169-182, 2009.

1416 Hanna, E., Cappelen, J., Fettweis, X., Mernild, S. H., Mote, T. L., Mottram, R., Steffen, K., Ballinger, T. J., and
 1417 Hall, R.: Greenland surface air temperature changes from 1981 to 2019 and implications for ice-sheet melt
 1418 and mass-balance change, *International Journal of Climatology*, 41, E1336-E1352, 10.1002/joc.6771,
 1419 2021.

1420 Hayashi, M., Quinton, W. L., Pietroniro, A., and Gibson, J. J.: Hydrologic functions of wetlands in a discontinuous
 1421 permafrost basin indicated by isotopic and chemical signatures, *Journal of Hydrology*, 296, 81-97,
 1422 https://doi.org/10.1016/j.jhydrol.2004.03.020, 2004.

1423 Hiyama, T., Asai, K., Kolesnikov, A. B., Gagarin, L. A., and Shepelev, V. V.: Estimation of the residence time
 1424 of permafrost groundwater in the middle of the Lena River basin, eastern Siberia, *Environmental Research
 1425 Letters*, 8, 10.1088/1748-9326/8/3/035040, 2013.

1426 Jasechko, S., Kirchner, J. W., Welker, J. M., and McDonnell, J. J.: Substantial proportion of global streamflow
 1427 less than three months old, *Nature Geoscience*, 9, 126-+, 10.1038/ngeo2636, 2016.

1428 Jessen, S., Holmslykke, H. D., Rasmussen, K., Richardt, N., and Holm, P. E.: Hydrology and pore water chemistry
 1429 in a permafrost wetland, Ilulissat, Greenland, *Water Resources Research*, 50, 4760-4774,
 1430 https://doi.org/10.1002/2013WR014376, 2014.

1431 Johansson, E., Gustafsson, L.-G., Berglund, S., Lindborg, T., Selroos, J.-O., Claesson Liljedahl, L., and Destouni,
 1432 G.: Data evaluation and numerical modeling of hydrological interactions between active layer, lake and
 1433 talik in a permafrost catchment, Western Greenland, *Journal of Hydrology*, 527, 688-703, 2015a.

1434 Johansson, E., Berglund, S., Lindborg, T., Petrone, J., van As, D., Gustafsson, L.-G., Näslund, J.-O., and Laudon,
 1435 H.: Hydrological and meteorological investigations in a periglacial lake catchment near Kangerlussuaq,
 1436 west Greenland – presentation of a new multi-parameter dataset, *Earth System Science Data*, 7, 93-108,
 1437 2015b.

1438 Johnson, C. E., Driscoll, C. T., Siccama, T. G., and Likens, G. E.: Element fluxes and landscape position in a
 1439 northern hardwood forest watershed ecosystem, *Ecosystems*, 3, 159-184, 2000.

1440 Juhls, B., Stedmon, C. A., Morgenstern, A., Meyer, H., Hölemann, J., Heim, B., Povazhnyi, V., and Overduin, P.
 1441 P.: Identifying Drivers of Seasonality in Lena River Biogeochemistry and Dissolved Organic Matter
 1442 Fluxes, *Frontiers in Environmental Science*, 8, 10.3389/fenvs.2020.00053, 2020.

1444 Jutebring Sterte, E., Johansson, E., Sjöberg, Y., Karlsen, R. H., and Laudon, H.: Groundwater-surface water
 1445 interactions across scales in a boreal landscape investigated using a numerical modelling approach, *Journal
 1446 of Hydrology*, 560, 184-201, 10.1016/j.jhydrol.2018.03.011, 2018.

1447 Jutebring Sterte, E., Lidman, F., Lindborg, E., Sjöberg, Y., and Laudon, H.: How catchment characteristics
 1448 influence hydrological pathways and travel times in a boreal landscape, *Hydrol. Earth Syst. Sci.*, 25, 2133-
 1449 2158, 10.5194/hess-25-2133-2021, 2021a.

1450 Jutebring Sterte, E., Lidman, F., Sjöberg, Y., Ploum, S. W., and Laudon, H.: Groundwater travel times predict
 1451 DOC in streams and riparian soils across a heterogeneous boreal landscape, *Science of the Total
 1452 Environment*, 849, 10.1016/j.scitotenv.2022.157398, 2022.

1453 Jutebring Sterte, E., Lidman, F., Balbarini, N., Lindborg, E., Sjöberg, Y., Selroos, J.-O., and Laudon, H.:
 1454 Hydrological control of water quality – Modelling base cation weathering and dynamics across
 1455 heterogeneous boreal catchments, *Science of The Total Environment*, 799, 149101,
 1456 <https://doi.org/10.1016/j.scitotenv.2021.149101>, 2021b.

1457 Koch, J. C., Connolly, C. T., Baughman, C., Repasch, M., Best, H., and Hunt, A.: The dominance and growth of
 1458 shallow groundwater resources in continuous permafrost environments, *Proc. Natl. Acad. Sci. U. S. A.*,
 1459 121, 10.1073/pnas.2317873121, 2024.

1460 Lachniet, M. S., Lawson, D. E., Stephen, H., Sloat, A. R., and Patterson, W. P.: Isoscapes of $\delta^{18}\text{O}$ and $\delta^2\text{H}$ reveal
 1461 climatic forcings on Alaska and Yukon precipitation, *Water Resources Research*, 52, 6575-6586,
 1462 <https://doi.org/10.1002/2016WR019436>, 2016.

1463 Laudon, H., Köhler, S., and Buffam, I.: Seasonal TOC export from seven boreal catchments in northern Sweden,
 1464 *Aquatic Sciences*, 66, 223-230, 2004.

1465 Laudon, H., Spence, C., Buttle, J., Carey, S. K., McDonnell, J. J., McNamara, J. P., Soulsby, C., and Tetzlaff, D.:
 1466 Save northern high-latitude catchments, *Nature Geoscience*, 10, 324-325, 10.1038/ngeo2947, 2017.

1467 Lebedeva, L.: Tracing surface and ground water with stable isotopes in a small permafrost research catchment,
 1468 E3S Web Conf., 98, 12011, 2019.

1469 Lidman, F., Boily, A., Laudon, H., and Kohler, S. J.: From soil water to surface water - how the riparian zone
 1470 controls element transport from a boreal forest to a stream, *Biogeosciences*, 14, 3001-3014, 10.5194/bg-
 1471 14-3001-2017, 2017.

1472 Lidman, F., Köhler, S. J., Mört, C.-M., and Laudon, H.: Metal Transport in the Boreal Landscape—The Role of
 1473 Wetlands and the Affinity for Organic Matter, *Environmental Science & Technology*, 48, 3783-3790,
 1474 10.1021/es4045506, 2014.

1475 Lindborg, T., Rydberg, J., Andersson, E., Löfgren, A., Lindborg, E., Saetre, P., Sohlenius, G., Berglund, S.,
 1476 Kautsky, U., and Laudon, H.: A carbon mass-balance budget for a periglacial catchment in West Greenland
 1477 – Linking the terrestrial and aquatic systems, *Science of The Total Environment*, 711, 134561,
 1478 <https://doi.org/10.1016/j.scitotenv.2019.134561>, 2020.

1479 Lindborg, T., Rydberg, J., Tröjbom, M., Berglund, S., Johansson, E., Löfgren, A., Saetre, P., Nordén, S.,
 1480 Sohlenius, G., Andersson, E., Petrone, J., Borgiel, M., Kautsky, U., and Laudon, H.: Biogeochemical data
 1481 from terrestrial and aquatic ecosystems in a periglacial catchment, West Greenland, *Earth Syst. Sci. Data*,
 1482 8, 439-459, 10.5194/essd-8-439-2016, 2016.

1483 Lockwood, P. V., McGarity, J. W., and Charley, J. L.: Measurement of chemical weathering rates using natural
 1484 chloride as a tracer, *Geoderma*, 64, 215-232, [https://doi.org/10.1016/0016-7061\(94\)00010-8](https://doi.org/10.1016/0016-7061(94)00010-8), 1995.

1485 Lyon, S. W., Morth, M., Humborg, C., Giesler, R., and Destouni, G.: The relationship between subsurface
 1486 hydrology and dissolved carbon fluxes for a sub-arctic catchment, *Hydrol. Earth Syst. Sci.*, 14, 941-950,
 1487 10.5194/hess-14-941-2010, 2010a.

1488 Lyon, S. W., Laudon, H., Seibert, J., Mört, M., Tetzlaff, D., and Bishop, K. H.: Controls on snowmelt water
 1489 mean transit times in northern boreal catchments, *Hydrol. Process.*, 24, 1672-1684, 10.1002/hyp.7577,
 1490 2010b.

1491 O'Connor, M. T., Cardenas, M. B., Neilson, B. T., Nicholaides, K. D., and Kling, G. W.: Active Layer
 1492 Groundwater Flow: The Interrelated Effects of Stratigraphy, Thaw, and Topography, *Water Resources
 1493 Research*, 55, 6555-6576, <https://doi.org/10.1029/2018WR024636>, 2019.

1494 Penna, D., Stenni, B., Šanda, M., Wrede, S., Bogaard, T. A., Gobbi, A., Borga, M., Fischer, B. M. C., Bonazza,
 1495 M., and Chárová, Z.: On the reproducibility and repeatability of laser absorption spectroscopy
 1496 measurements for $\delta^{18}\text{H}$ and $\delta^{18}\text{O}$ isotopic analysis, *Hydrol. Earth Syst. Sci.*, 14,
 1497 1551-1566, 10.5194/hess-14-1551-2010, 2010.

1498 Petrone, J., Sohlenius, G., Johansson, E., Lindborg, T., Näslund, J. O., Strömgren, M., and Brydsten, L.: Using
 1499 ground-penetrating radar, topography and classification of vegetation to model the sediment and active
 1500 layer thickness in a periglacial lake catchment, western Greenland, *Earth Syst. Sci. Data*, 8, 663-677,
 1501 10.5194/essd-8-663-2016, 2016.

1502 Quinton, W. L. and Porneroy, J. W.: Transformations of runoff chemistry in the Arctic tundra, Northwest
 1503 Territories, Canada, *Hydrol. Process.*, 20, 2901-2919, 2006.

1504 Rantanen, M., Karpechko, A. Y., Lipponen, A., Nordling, K., Hyvärinen, O., Ruosteenoja, K., Vihma, T., and
 1505 Laaksonen, A.: The Arctic has warmed nearly four times faster than the globe since 1979, *Communications*
 1506 *Earth & Environment*, 3, 10.1038/s43247-022-00498-3, 2022.

1507 Ross, C. A., Ali, G., Bansah, S., and Laing, J. R.: Evaluating the Relative Importance of Shallow Subsurface Flow
 1508 in a Prairie Landscape, *Vadose Zone Journal*, 16, 10.2136/vzj2016.10.0096, 2017.

1509 Rydberg, J., Lindborg, T., Sølenius, G., Reuss, N., Olsen, J., and Laudon, H.: The importance of eolian input on
 1510 lake-sediment geochemical-composition in the dry proglacial landscape of western Greenland., *Arct.*
 1511 *Antarct. Alp. Res.*, 48, 93-109, 10.1657/AAAR0015-009, 2016.

1512 Rydberg, J., Lindborg, T., Lidman, F., Tröjbom, M., Berglund, S., Lindborg, E., Kautsky, U., and Laudon, H.:
 1513 Biogeochemical cycling in a periglacial environment – A multi-element mass-balance budget for a
 1514 catchment in West Greenland, *CATENA*, 231, 107311, <https://doi.org/10.1016/j.catena.2023.107311>,
 1515 2023.

1516 Sjöberg, Y., Coon, E., Sannel, A. B. K., Pannetier, R., Harp, D., Frampton, A., Painter, S. L., and Lyon, S. W.:
 1517 Thermal effects of groundwater flow through subarctic fens: A case study based on field observations and
 1518 numerical modeling, *Water Resources Research*, 52, 1591-1606, 10.1002/2015wr017571, 2016.

1519 Sodemann, H., Masson-Delmotte, V., Schwierz, C., Vinther, B. M., and Wernli, H.: Interannual variability of
 1520 Greenland winter precipitation sources: 2. Effects of North Atlantic Oscillation variability on stable
 1521 isotopes in precipitation, *Journal of Geophysical Research: Atmospheres*, 113,
 1522 <https://doi.org/10.1029/2007JD009416>, 2008.

1523 Sprenger, M., Stumpf, C., Weiler, M., Aeschbach, W., Allen, S. T., Benettin, P., Dubbert, M., Hartmann, A.,
 1524 Hrachowitz, M., Kirchner, J. W., McDonnell, J. J., Orlowski, N., Penna, D., Pfahl, S., Rinderer, M.,
 1525 Rodriguez, N., Schmidt, M., and Werner, C.: The Demographics of Water: A Review of Water Ages in
 1526 the Critical Zone, *Rev. Geophys.*, 57, 800-834, 10.1029/2018rg000633, 2019.

1527 Stewart, B., Shanley, J. B., Kirchner, J. W., Norris, D., Adler, T., Bristol, C., Harpold, A. A., Perdrial, J. N., Rizzo,
 1528 D. M., Sterle, G., Underwood, K. L., Wen, H., and Li, L.: Streams as Mirrors: Reading Subsurface Water
 1529 Chemistry From Stream Chemistry, *Water Resources Research*, 58, e2021WR029931,
 1530 <https://doi.org/10.1029/2021WR029931>, 2022.

1531 Tetzlaff, D., Piovano, T., Ala-Aho, P., Smith, A., Carey, S. K., Marsh, P., Wookey, P. A., Street, L. E., and
 1532 Soulsby, C.: Using stable isotopes to estimate travel times in a data-sparse Arctic catchment: Challenges
 1533 and possible solutions, *Hydrol. Process.*, 32, 1936-1952, 10.1002/hyp.13146, 2018.

1534 Throckmorton, H. M., Newman, B. D., Heikoop, J. M., Perkins, G. B., Feng, X. H., Graham, D. E., O'Malley, D.,
 1535 Vesselinov, V. V., Young, J., Wullschleger, S. D., and Wilson, C. J.: Active layer hydrology in an arctic
 1536 tundra ecosystem: quantifying water sources and cycling using water stable isotopes, *Hydrol. Process.*, 30,
 1537 4972-4986, 10.1002/hyp.10883, 2016.

1538 van Gool, J., Marker, M., and Mengel, F.: The palaeoproterozoic Nagssugtoqidian orogen in West Greenland:
 1539 current status of work by the Danish lithosphere centre, *Bulletin Grønlands Geologiske Undersøgelse*, 172,
 1540 88-94, 1996.

1541 Vonk, J. E., Tank, S. E., Bowden, W. B., Laurion, I., Vincent, W. F., Alekseychik, P., Amyot, M., Billet, M. F.,
 1542 Canario, J., Cory, R. M., Deshpande, B. N., Helbig, M., Jammet, M., Karlsson, J., Larouche, J., MacMillan,
 1543 G., Rautio, M., Anthony, K. M. W., and Wickland, K. P.: Reviews and syntheses: Effects of permafrost
 1544 thaw on Arctic aquatic ecosystems, *Biogeosciences*, 12, 7129-7167, 10.5194/bg-12-7129-2015, 2015.

1545 Walvoord, M. A. and Kurylyk, B. L.: Hydrologic Impacts of Thawing Permafrost-A Review, *Vadose Zone*
 1546 *Journal*, 15, 10.2136/vzj2016.01.0010, 2016.

1547 Wang, S. Y., He, X. B., Kang, S. C., Fu, H., and Hong, X. F.: Estimation of stream water components and
 1548 residence time in a permafrost catchment in the central Tibetan Plateau using long-term water stable
 1549 isotopic data, *Cryosphere*, 16, 5023-5040, 10.5194/tc-16-5023-2022, 2022.

1550 Wilcox, E. J., Wolfe, B. B., and Marsh, P.: Assessing the influence of lake and watershed attributes on snowmelt
 1551 bypass at thermokarst lakes, *Hydrol. Earth Syst. Sci.*, 26, 6185-6205, 10.5194/hess-26-6185-2022, 2022.

1552 Williams, M. W., Hood, E., Molotch, N. P., Caine, N., Cowie, R., and Liu, F. J.: The 'teflon basin' myth: hydrology
 1553 and hydrochemistry of a seasonally snow-covered catchment, *Plant Ecology & Diversity*, 8, 639-661,
 1554 10.1080/17550874.2015.1123318, 2015.

1555 Winnick, M. J., Carroll, R., Williams, K., Maxwell, R., Dong, W., and Maher, K.: Snowmelt controls on
 1556 concentration-discharge relationships and the balance of oxidative and acid-base weathering fluxes in an
 1557 alpine catchment, East River, Colorado, *Water Resources Research*, n/a-n/a, 10.1002/2016WR019724,
 1558 2017.

1559 Zastruzny, S. F., Sjöberg, Y., Jensen, K. H., Liu, Y. J., and Elberling, B.: Impact of Summer Air Temperature on
 1560 Water and Solute Transport on a Permafrost-Affected Slope in West Greenland, *Water Resources*
 1561 *Research*, 60, 10.1029/2023wr036147, 2024.

1562

▼
▲ **Page 22: [6] Deleted** Microsoft Office User 18/11/2025 11:02:00

▼
▲ **Page 22: [6] Deleted** Microsoft Office User 18/11/2025 11:02:00

▼
▲ **Page 22: [6] Deleted** Microsoft Office User 18/11/2025 11:02:00

▼
▲ **Page 22: [6] Deleted** Microsoft Office User 18/11/2025 11:02:00

▼
▲ **Page 22: [6] Deleted** Microsoft Office User 18/11/2025 11:02:00

▼
▲ **Page 22: [6] Deleted** Microsoft Office User 18/11/2025 11:02:00

▼
▲ **Page 22: [6] Deleted** Microsoft Office User 18/11/2025 11:02:00

▼
▲ **Page 22: [6] Deleted** Microsoft Office User 18/11/2025 11:02:00

▼
▲ **Page 22: [6] Deleted** Microsoft Office User 18/11/2025 11:02:00

▼
▲ **Page 22: [6] Deleted** Microsoft Office User 18/11/2025 11:02:00

▼
▲ **Page 22: [6] Deleted** Microsoft Office User 18/11/2025 11:02:00